Research Article

Late glacial to Holocene fluvial dynamics in the Upper Rhine alluvial plain, France

Mubarak Abdulkarim[a] (iD), Laurent Schmitt[b] (iD), Alexander Fülling[a] (iD), Claire Rambeau[b] (iD), Damien Ertlen[b] (iD), Daniela Mueller[a] (iD), Stoil Chapkanski[c,d] and Frank Preusser[a] (iD)

[a]Institute of Earth and Environmental Science, University of Freiburg, Freiburg, Germany; [b]Laboratoire Image, Ville, Environnement (LIVE UMR 7362), CNRS/Université de Strasbourg/ENGEES, Strasbourg, France; [c]University of Rouen Normandy, IDEES Laboratory, UMR 6266, CNRS, 17 Rue Lavoisier, 76821, Mont Saint-Aignan, France and [d]Laboratoire de Géographie Physique (UMR-8591), CNRS/Université Paris 1, Thiais, France

Abstract

High-resolution sedimentological and geochronological investigations of paleochannel systems in the Ried Central d'Alsace (northeastern France) allow for the reconstruction of the late glacial and Holocene fluvial evolution of this section of the Upper Rhine alluvial plain. During the Oldest Dryas, the landscape featured a dominant braided Rhine system and, to a lesser extent, a braided Fecht system. The shift to the Bølling-Allerød saw a narrowing of the Rhine's active channel belt, the development of a complex channel pattern, and the genesis of the Ill River. The river channel patterns remained unchanged during the Younger Dryas. In the Early Holocene, the Rhine's active belt narrowed further, and the Rhine and Ill Rivers developed braided-anastomosing and anastomosing channel patterns, respectively. Throughout the Holocene, both rivers maintained their channel patterns while migrating east and west across the alluvial plain, respectively. In the late glacial, fluvial dynamics in this section of the Upper Rhine plain were primarily influenced by climate-related environmental and hydrogeomorphological changes. Conversely, during the Holocene, the evolution of the fluvial hydrosystems was driven by a complex interaction of climatic and non-climatic factors, including human activity at the catchment scale, alluvial plain architecture, and local neotectonics.

Keywords: Upper Rhine plain, Fluvial dynamics, late glacial, Holocene, Paleochannels, Anastomosing channels, Rhine River, Ill River, Fecht River

Introduction

Fluvial systems occupy a key position in paleoenvironmental research, providing important archives of environmental and geomorphic changes, especially during the late Pleistocene and Holocene (e.g., Arbogast et al., 2008; Zielhofer et al., 2008; Kirchner et al., 2015, 2022; von Suchodoletz et al., 2015; Depreux et al., 2021). In the last century, global climatic changes and increased human pressure on fluvial systems and their catchments have spurred interest in understanding the long-term dynamics of fluvial systems, particularly during the late Pleistocene and the Holocene. These time periods are critical and of significant interest, as they marked a transition from the cold conditions of the last ice age to the warmer conditions of the Holocene, which was characterized by significant changes such as glacial retreats, hydro-climatic and environmental shifts, and changing sedimentation conditions (Lowe and Walker, 2014; Druzhinina et al., 2020). Moreover, human activities such

as agriculture, industrialization, and settlement expansion had a significant impact on the environment and landscapes during these phases (Kalis et al., 2003; Lang et al., 2003; Houben et al., 2006; Mäckel et al., 2009).
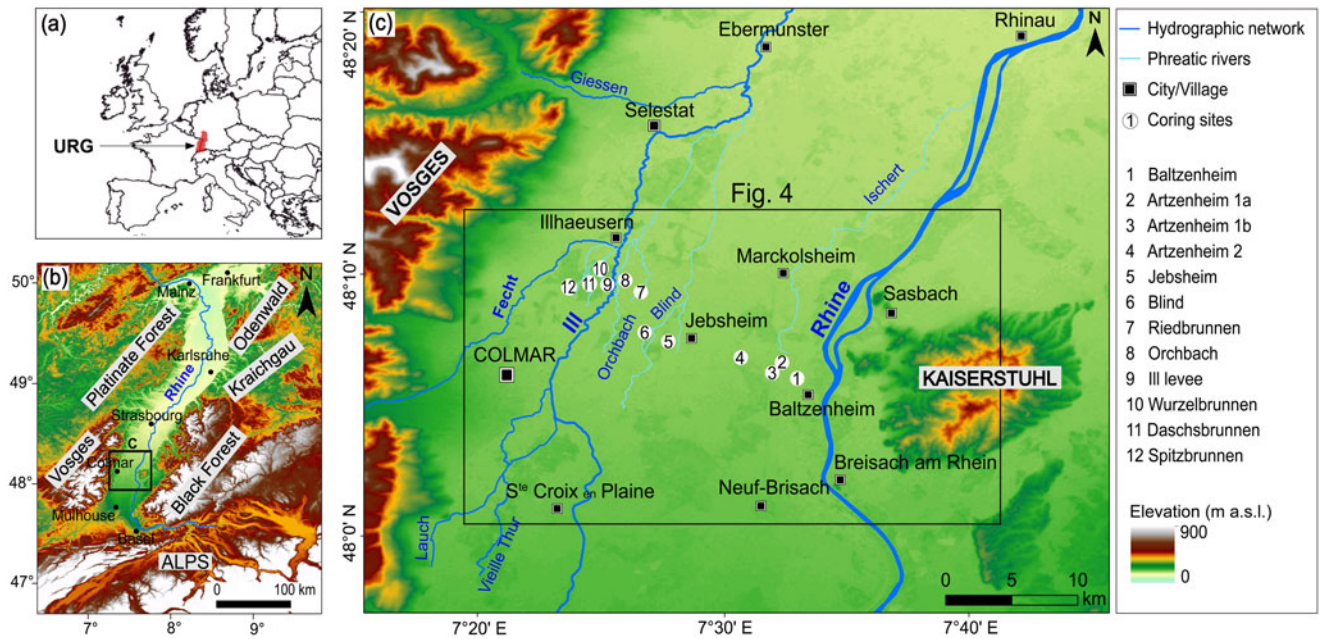
The Rhine fluvial hydrosystem in northwest Europe, like many other fluvial systems in the northern temperate zone, underwent a series of adaptive modifications in its functioning and morphodynamics in response to late Pleistocene and Holocene climate and environmental changes (Berendsen et al., 1995; Dambeck and Thiemeyer, 2002; Schirmer et al., 2005; Bos et al., 2008; Erkens et al., 2011; Schmitt et al., 2016). Thus, the Rhine system has been the subject of extensive research to comprehend the interplay between natural and anthropogenic factors and their impact on the long- and short-term evolution of fluvial systems and their associated landscapes (e.g., Törnqvist, 1994, 1998; Stouthamer and Berendsen, 2000; Dambeck and Thiemeyer, 2002; Lang et al., 2003; Kasse et al., 2005; Houben et al., 2006; Erkens et al. 2009, 2011; Lämmermann-Barthel et al., 2009; Schmitt et al., 2016). However, despite this body of research, relatively few studies have focused on understanding the long-term fluvial evolution of the Upper Rhine alluvial plain, a densely populated section along the Rhine between Basel (Switzerland) and Bingen (Germany; Fig. 1).

Figure 1. Overview of the study area. (**a**) Location map of the Upper Rhine Graben (URG) in Europe. (**b**) Location of the study area within the URG. (**c**) The investigation area (framed by the black box) within the French Rhine alluvial plain showing the locations of coring sites. Source of digital elevation data: CGIAR-CSI (n.d., https://srtm.csi.cgiar.org/srtmdata).

While some studies have been undertaken in the northern reaches of the Upper Rhine plain, between Karlsruhe and Mainz (e.g., Dambeck and Thiemeyer, 2002; Bos et al., 2008; Erkens et al., 2009, 2011; Fig. 1), studies of comparable scope in the southern and central parts of the plain, between Basel and Karlsruhe, are relatively scarce, with only a few exceptions (e.g., Carbiener, 1969; Al Siddik, 1986; Hirth, 1971; Schmitt et al., 2016). Most studies conducted in this part of the Upper Rhine plain have focused on the historical fluvial dynamics or have been restricted to specific aspects such as neotectonics, historical flooding patterns, or human impacts on river dynamics (e.g., Lang et al., 2003; Ollive et al., 2006; Boës et al., 2007; Lämmermann Barthel et al., 2009; Mäckel et al., 2009; Eschbach et al., 2018). Few paleoenvironmental studies have been conducted in recent years to gain a deeper understanding of the Holocene evolution of the Upper Rhine fluvial hydrosystem, with a particular focus on the Ried Central d'Alsace region (located between Colmar and Strasbourg) within the French Upper Rhine plain (e.g., Boës et al., 2007; Schmitt et al., 2016; Chapkanski et al., 2020; Abdulkarim et al., 2022). This area is an extensive and exceptionally biodiverse alluvial landscape (Carbiener, 1983a, 1983b) that features a remarkably well-preserved and complex network of paleochannels, providing an ideal and regionally significant fluvial archive for deciphering the long-term fluvial dynamics and evolution of the southern and central parts of Upper Rhine plain.

Preliminary studies indicate the presence of at least five major paleochannel systems in the region, with considerable differences in their surface topographic features, geometry and architecture, and provenance of infill sediments (Abdulkarim et al., 2022). These differences in geomorphic features and sediment provenance are linked to significant shifts in hydro-geomorphological processes in the area, as well as lateral movements of the Rhine and Ill Rivers (the latter is a major tributary of the Rhine in the region; Fig. 1), which are believed to have persisted since at least the Early Holocene (e.g., Schmitt et al., 2016; Abdulkarim

et al., 2022). However, these previous studies primarily relied on remote sensing data, hand-augured core sediment profiles, and very few radiocarbon ages. As a result, the sedimentological characteristics of the paleochannel systems remain poorly understood, and there are still significant ambiguities regarding the rivers' evolutionary trajectories and lateral shifting patterns, as well as the timing of major shifting episodes. Moreover, the factors governing the lateral movements of rivers in the region have yet to be definitively established.

In view of this knowledge gap, the work presented here aims to reconstruct the late glacial and Holocene evolution of the fluvial hydrosystems in the Ried Central d'Alsace, particularly focusing on (1) the major fluvial system changes, especially the lateral mobility of the fluvial hydrosystems; and (2) their controlling factors. Objectives of this study are to: (1) systematically characterize the infill sediments of the paleochannels and natural levee of the Ill River using a multiproxy approach including sedimentological, geochemical, and geochronological methods; (2) accurately reconstruct the temporal trajectories of the rivers and establish a robust chronology of the fluvial system changes since the late glacial period; and (3) assess potential driving factors that controlled major fluvial system changes, lateral river movements, and subsequent paleochannel formation.

Geologic and Geomorphological Setting

The study area is located within the southern part of the Upper Rhine Graben (URG), on the French side of the Rhine alluvial plain (Fig. 1). As part of the European Cenozoic Rift System (Ziegler, 1992), the URG is a rift valley measuring 300 km in length and 30–40 km in width, extending from the Jura Mountains in the south/southwest to the Rhenish Massif in the north. To the west, the URG is bordered by the Vosges Massif and Palatinate Forest, and on its eastern periphery by the Black Forest and Odenwald Mountains, which are separated by the Kraichgau depression.
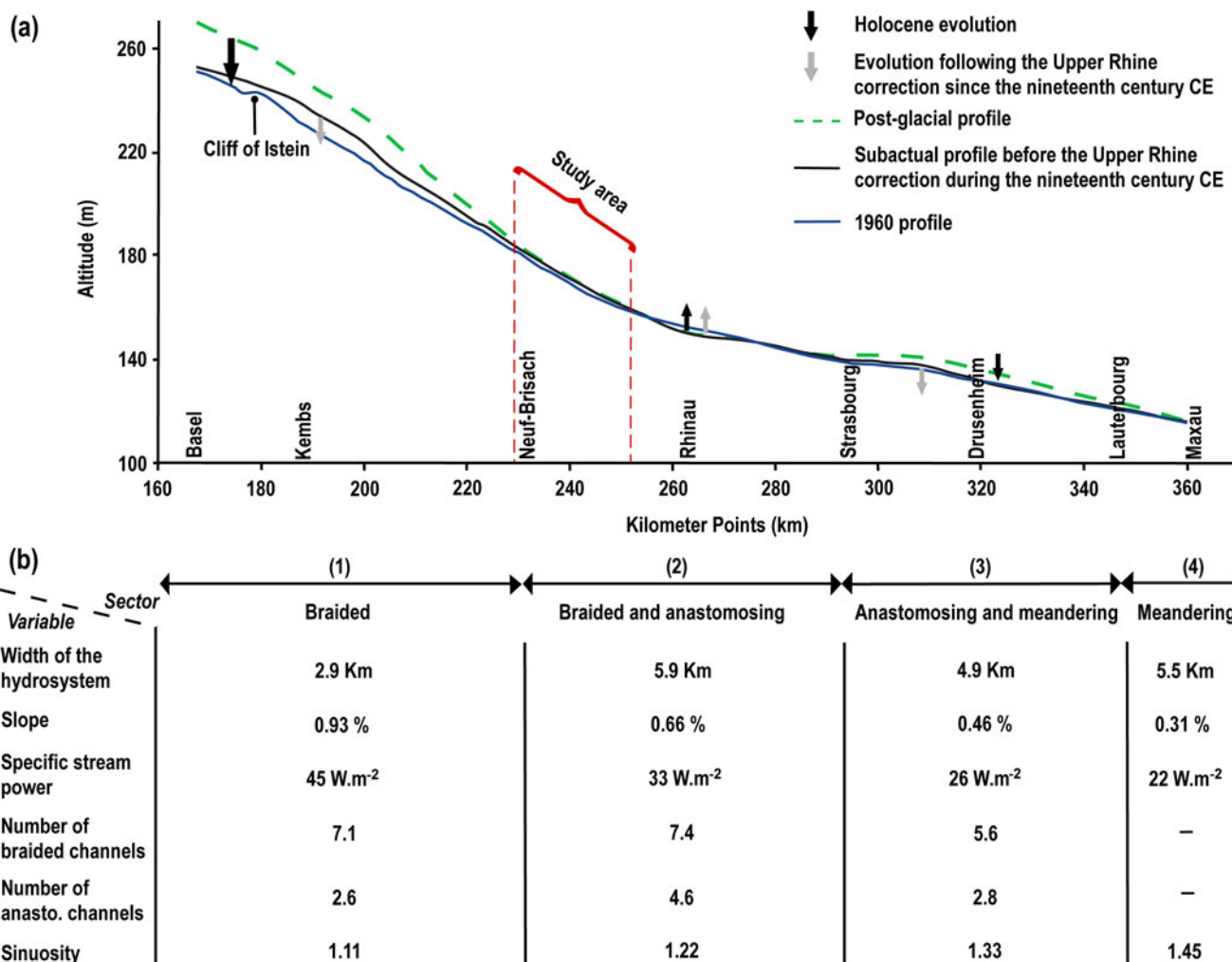
The graben shoulders are formed mainly of Variscian crystalline basement and Mesozoic siliciclastic and carbonate sedimentary rocks (Fig. 1). Since the beginning of the Pleistocene, the Rhine has flowed toward the North Sea through the subsiding URG basin (Preusser, 2008), which serves as a major sediment depocenter with accumulations reaching several hundred of meters in thickness (e.g., Haimberger et al., 2005; Gabriel et al., 2013).

At the end of the late glacial, the Rhine's longitudinal profile evolved due to factors such as decreased water and sediment volume caused by warmer climatic conditions, sediment entrapment in Swiss Rhine lakes, and neotectonic movements (Schmitt et al., 2016 and references therein). Consequently, the Upper Rhine's longitudinal profile incised in some sections during the Holocene, particularly from Basel to Neuf-Brisach and from Strasbourg to Lauterbourg, while other sections (Neuf-Brisach to Strasbourg) remained stable or slightly elevated (Carbiener, 1969, 1983b; Fig. 2).

As a result, the Holocene Upper Rhine and its alluvial plain are divided into four longitudinal sectors (Fig. 2), as delineated by Carbiener (1969, 1983b) and Schmitt et al. (2016). The upstream sector, from Basel to Neuf-Brisach, is characterized by a preponderance of braided channel patterns with some anastomosing and closed anabranching channels (Arnaud, 2012; Schmitt et al., 2016). The median sector, between Neuf-Brisach and Strasbourg, exhibits a braided-anastomosing pattern, while the downstream sector, from Strasbourg to Lauterbourg, combines anastomosing channels and incipient meanders. A dominant meandering pattern typifies the sector farther north (downstream), from Lauterbourg to Bingen. It is important to highlight that river engineering works in the nineteenth and twentieth centuries have destroyed these natural channel patterns and dynamics of the Upper Rhine (e.g., Preusser et al., 2016; Eschbach et al., 2018).

The French Rhine alluvial plain is typically divided into two distinct longitudinal geomorphic zones, the "Hardt" and the "Ried," based on hydrological, ecological, and pedogenic differences (Carbiener, 1969; Hirth, 1971; Kremer et al., 1978; Ollive et al., 2006; Fig. 3). The Hardt zone (corresponding mostly to the Rhine braided sector) is characterized by coarse sand and gravel islands formed as part of the Rhine River's Pleistocene alluvial terraces. This zone is further subdivided into the Hardt Rouge and Hardt Grise. The Ried area (corresponding mostly to the Rhine braided-anastomosing sector) is a low-lying, marshy landscape with hydromorphic soils, predominantly composed of mud and fine sand interspersed with organic matter (OM; Carbiener, 1969, 1983b; Hirth, 1971; Kremer et al., 1978; Ollive et al., 2006). The Ried is transversely subdivided into four sections within the alluvial plain: Ried Gris, Ried Noir, Ried Blond, and Ried Brun (Fig. 3).

Sector Variable	(1) Braided	(2) Braided and anastomosing	(3) Anastomosing and meandering	(4) Meandering
Width of the hydrosystem	2.9 Km	5.9 Km	4.9 Km	5.5 Km
Slope	0.93 %	0.66 %	0.46 %	0.31 %
Specific stream power	45 W.m^{-2}	33 W.m^{-2}	26 W.m^{-2}	22 W.m^{-2}
Number of braided channels	7.1	7.4	5.6	—
Number of anasto. channels	2.6	4.6	2.8	—
Sinuosity	1.11	1.22	1.33	1.45

Figure 2. (**a**) Postglacial and Holocene longitudinal profiles of the Upper Rhine. (**b**) Some Upper Rhine hydromorphological characteristics for each longitudinal sector (modified from Commission Internationale de l'Hydrologie du Bassin du Rhin, 1977; Carbiener and Dillmann, 1992; Schmitt, 2001; Schmitt et al., 2019).
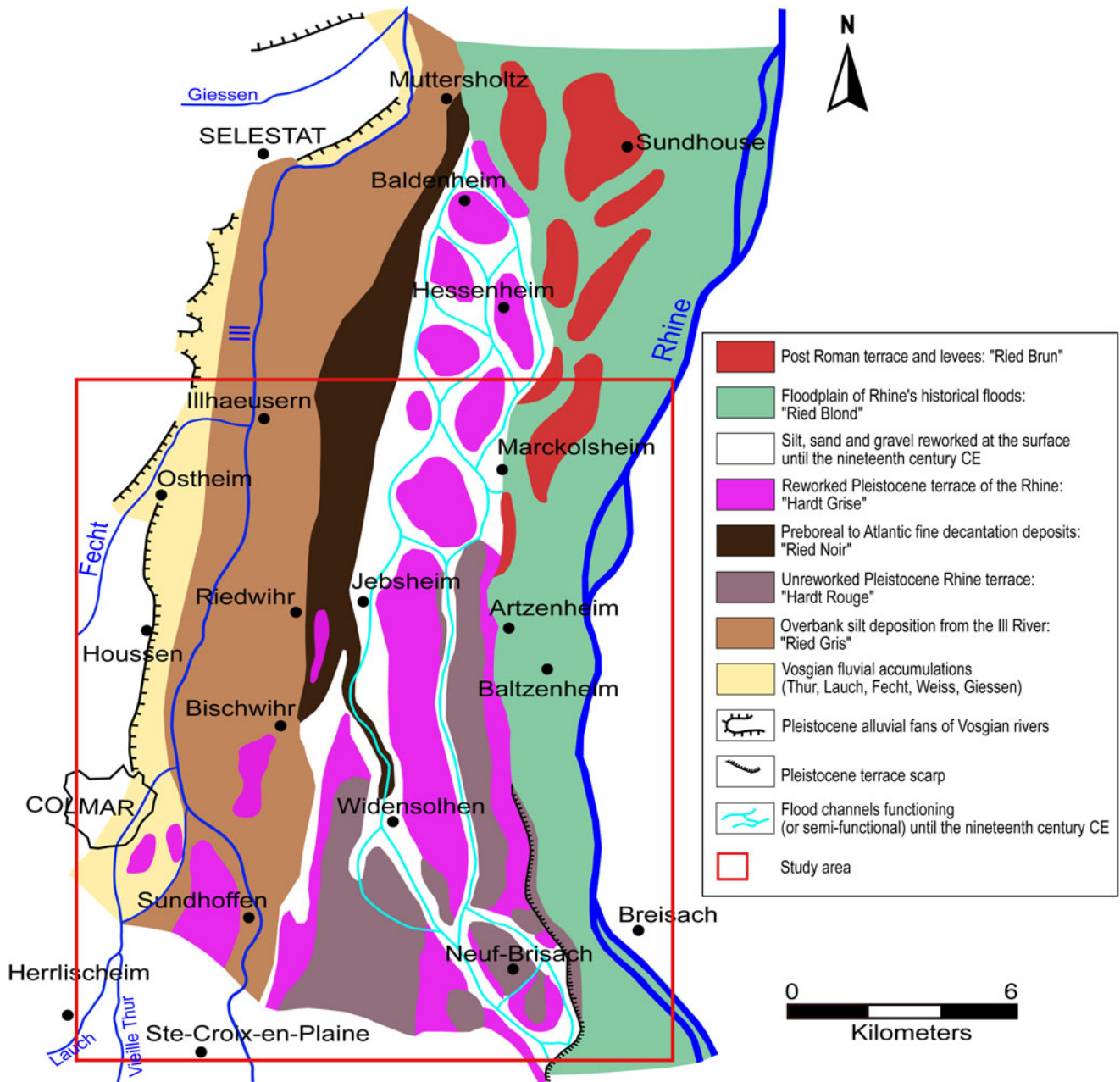
Figure 3. Geomorphological map of a section of the French Rhine alluvial plain (Colmar-Sélestat; according to Hirth [1971], revised by Schmitt [2001] and Schmitt et al. [2016]), the southern portion of which constitutes our study area. Figure modified from Schmitt et al. (2016).

The study area is located in the valley region between Illhaeusern and Marckolsheim in the north and Neuf-Brisach and Sainte-Croix-en Plaine in the south (Figs. 1 and 3). It covers an area of approximately 572 km² and is part of the alluvial plain's braided-anastomosing sector. The area also forms the southern portion of the Ried Central d'Alsace. The Rhine River mainly drains the area in the east and the Ill River in the west. The Fecht River, which flows into the Ill River at Illhaeusern, is a major western tributary in this region.

The contemporary floodplain has a distinct microtopography characterized by a dense and intricate network of paleochannels (Fig. 4) filled with a mix of clastic and organic deposits several meters thick (Schmitt et al., 2007, 2011, 2016; Chapkanski et al., 2020; Abdulkarim et al., 2022). Some of these paleochannels,

however, have a current connection to groundwater or the Rhine (during floods) or the Ill River and contain phreatic and semi-phreatic rivers that are home to a diverse range of aquatic macrophytes (Carbiener, 1983a, 1983b; Trémolières et al., 1993; Schmitt, 2001; Schmitt et al., 2016). The paleochannels show distinct differences in their surface topographic features and paleo-flow orientations (Abdulkarim et al., 2022; Fig. 4).

Methods

Core sampling

Eleven paleochannels within the alluvial plain and the natural levee of the Ill River were selected for this study (Figs. 1 and 4).
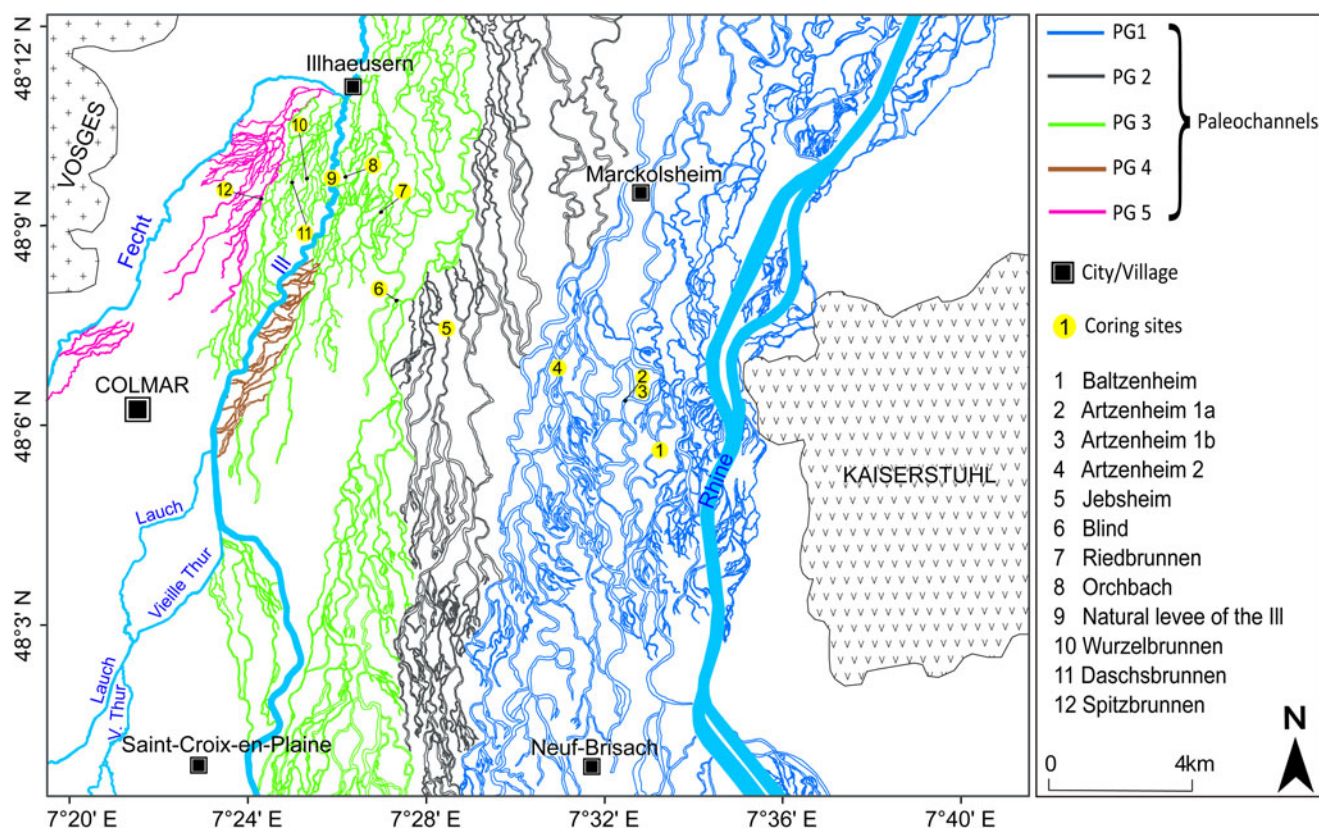
Figure 4. Map illustrating the paleochannel network in the study area and the spatial demarcation of five paleochannel groups (PG 1 to PG 5) according to Abdulkarim et al. (2022). PG 1, Holocene Rhine paleochannels; PG 2, late glacial braided Rhine paleochannels; PG 3, Ill paleochannels superimposed on late glacial Rhine paleochannels; PG 4, ancient flood channels of the Ill; PG 5, paleochannels of the Fecht system. Figure modified from Abdulkarim et al. (2022).

The selection technique aimed to cover a transect of paleochannels between the Rhine and the western side of the Ill River, as well as all paleochannel groups (PG) defined by Abdulkarim et al. (2022) (Fig. 4). However, no paleochannels from the PG 4 group (brown signature in Fig. 4) could be cored, as they are concealed by thick grassland and, in some areas, the artificial Ill River dikes. Paleochannels with active streams were named after their active streams, while those that were filled and showed no current water flow were termed according to their geographic positions.

Sediment cores were recovered from the paleochannels and natural levee of the Ill River using an electric-powered percussion hammer (Milwaukee K 2500 H) with a core sampler and opaque plastic liners (5 cm in diameter). Peat and organic-rich sediment units were also sampled for radiocarbon dating in the paleochannels of "Artzenheim 1," "Daschsbrunnen," and "Spitzbrunnen," respectively, using a Russian peat corer.

Sediment analyses

The sediment cores were split lengthwise into reference and working core halves in the laboratory under subdued red light. The reference core halves were immediately wrapped in light-blocking material for luminescence dating, while the working halves were utilized for sedimentological and geochemical analyses. Before the analyses, working cores were photographed and systematically logged for properties such as color, texture, organic content, presence of plant macro-remains and shells, and gradations between units. Sediment subsamples were taken every ca. 10 cm while ensuring representation of each stratigraphic unit.

The OM content of the sediment samples was determined using the loss-on-ignition approach (cf. Heiri et al., 2001). Carbonate content was obtained by gasometric measurement, employing the "Karbonate-Bombe" technique (Müller and Gastner, 1971; Birch, 1981). Magnetic susceptibility (MS) was measured three times for each sample using a Bartington MS2 system equipped with an MS2K high-resolution surface sensor (Dearing, 1999). This method helped in the identification of distinct lithogenetic units.

Grain-size measurements utilized a Malvern Mastersizer 3000 laser particle size analyzer with a wet dispersion unit. Sample preparation and measurement procedures followed the protocol of Abdulkarim et al. (2021), and grain-size parameters (mean and sorting) were calculated using GRADISTAT v. 8.0 (Blott and Pye, 2001). The provenance of sediments was determined by combining mid-infrared spectroscopy (MIRS) and discriminant analysis (DA) (Supplementary Table S1). MIRS measurements were conducted on ground sediment samples using an FT-IR Frontier Spectrometer with a KBr beam splitter and diffuse reflectance sampling accessory, following protocols detailed by Ertlen et al. (2010), Chapkanski et al. (2020), and Abdulkarim et al. (2022). In this study, 63 provenance results from Abdulkarim et al. (2022) and 8 new samples from the natural levee of the Ill River were utilized (Supplementary Table S1).

Radiocarbon dating

Accelerator mass spectrometry (AMS) radiocarbon (^{14}C) dating was performed on 15 plant macrofossils at the Poznan

Radiocarbon Laboratory, Poland. The samples were pretreated with the acid–alkali–acid technique to remove undesirable elements (such as inorganic carbon and humic acids) and extract datable fractions. Radiocarbon ages (^{14}C BP) were calibrated using OxCal v. 4.4 (Bronk Ramsey, 2009) based on the IntCal 20 calibration curve (Reimer et al., 2020).

Infrared stimulated luminescence (IRSL) screening

For rapid, high-resolution semiquantitative chronological assessment, sediment samples from the light-sealed reference core halves were investigated using the IRSL screening technique. In this approach, the natural IRSL signal (L_n) of the dried bulk sediment is normalized by a subsequent test dose measurement (T_n). By applying the same test dose to all samples in this study, the ratio L_n/T_n provides information regarding the dose absorbed since burial. However, neither differences in dose rates nor correction for the signal loss commonly observed in feldspar (fading) are considered. Nevertheless, the received ratios represent a rough age assessment and highlight trends and changes in the rate of sedimentation (periods of continuous accumulation and breaks in deposition; Roberts et al., 2009; May et al., 2018; Schulze et al., 2022). Furthermore, this approach reveals indications for horizons where the IRSL signal was only partially reset at the time of deposition, for example, layers that were deposited by massive floods. Hence, this method was utilized as a complementary technique to help identify specific sedimentary units for proper luminescence dating and assist in a more effective sampling strategy.

Samples were collected at 10 cm intervals using microtubes (1 cm in diameter, 4 cm long). Subsequently, samples were dried at 50°C and gently homogenized to disperse the fine sediments. Three aliquots per sample were prepared on steel cups (1 cm diameter) coated with silicon oil (6 mm stamp). Luminescence measurements were performed on a Lexsyg Smart reader (Richter et al., 2015), using only the first cycle of the single-aliquot regenerative protocol (Murray and Wintle, 2000; Wintle and Murray, 2006). The measurement procedure follows a simplified IRSL sequence with stimulations at 50°C (Supplementary Table S2), only measuring the natural luminescence signal (L_n) and a test dose signal (T_n; 22 Gy). The L_n/T_n ratio was calculated for each sample using Risø Analyst v. 4.57.

Luminescence dating

Altogether, 49 samples were taken for luminescence dating with the sampling location determined based on stratigraphy and the results of IRSL screening. Samples were taken from the reference cores (as all other further steps under subdued red-light conditions) by avoiding the outer parts that may have been contaminated during the drilling and core opening. According to grain-size composition, either the coarse-grain (fine to medium sand) or fine-grain (fine silt) fraction was used (cf. Preusser et al., 2008). For the first, samples were wet sieved (100–200 μm), and the material obtained was subsequently treated with 20% HCl, 30% H_2O_2, and sodium oxalate to remove carbonates and OM and to disperse clay particles, respectively. Each step was followed by rinsing with de-ionized water. K-feldspar (δ < 2.58 g/cm³) and quartz (δ > 2.58 g/cm³, δ < 2.70 g/cm³) fractions were isolated using heavy liquid separation (sodium heteropolytungstates, LST FastFloat). For some of the samples, the quartz fraction was etched in 40% hydrofluoric acid for 60 min to remove the outer rim of the grain and any remaining feldspar contamination. However, test measurements revealed little to no response of the quartz to optical stimulation, in concert with observations for many other samples from the region (Preusser et al., 2016, 2021; unpublished data). Hence, measurements were limited to utilize the feldspar signal. Feldspar grains were fixed on stainless steel cups (Freiberg Instruments) using silicon oil (1 mm stamp; ca. 30 grains/cup) as adhesive.

For some of the samples, grain-size distribution revealed a very low abundance of sand grains in the sediment, in particular for overbank deposits and final-stage channel infills. For these samples, after the chemical treatment detailed earlier, the 4–11 μm fraction was enriched by settling following Stokes's law. The polymineral fraction was then placed on stainless steel disks of 10 mm diameter (fully covered).

Measurements were conducted on a Risø TL/OSL-DA-15C/D reader (controller model: DA-20; detection filter combination: Schott BG-39, Corning 7-59) using a modified version of the post-IR IRSL protocol (Buylaert et al., 2009; Supplementary Table S3), which uses a preheat of 270°C for 60 s followed by infrared stimulation at 50°C and a second infrared stimulation at 250°C. The two signals are recorded and referred to as IRSL and pIR, respectively. The signal of the first measurement (IRSL), is quickly reset by daylight but instable with time, a phenomenon known as fading. In the presence of fading, ages will be underestimated. To overcome this, measuring of the signal loss in the laboratory and extrapolating it to geologic times is required; however, this is not always straightforward. During the second stimulation at elevated temperature (pIR), a signal that is considered stable over long periods of time (not fading) is recorded, but it requires more time to be reset by daylight. An incompletely reset signal in the sample will result in overestimation of the pIR age. While a lower second stimulation temperature (225°C) is often applied, measurements were conducted following Faershtein et al. (2020), who demonstrated a high signal stability for the signal stimulated at 250°C. To test the suitability of this approach, dose-recovery tests were performed on coarse-grain feldspar of three samples (Spt-135 cm, Bz-80 cm, Ried-95 cm; three aliquots each) after signal reset (100 s infrared stimulation at 260°C carried out three times) and giving a beta dose of approximately 22 Gy. This dose could be determined with IRSL at 50°C as well as with pIR at 250°C within an error margin of 10% (ratio of measured to given dose: Spt-135 cm: IRSL: 0.94 ± 0.03, pIR: 0.94 ± 0.02; Bz-80 cm: IRSL: 1.0 ± 0.02, pIR: 0.9 ± 0.03; Ried-95 cm: IRSL: 1.07 ± 0.02, pIR: 1.02 ± 0.02). For fine grains, seven replicate measurements of equivalent dose (D_e) were carried out, while the number was increased to 16 for coarse grains. Mean D_e values for both approaches were calculated using the central age model (CAM), whereas the minimum age model (MAM; σ_b value = 0.10) was additionally applied only for coarse grains (Galbraith et al., 1999). The results are summarized in Supplementary Table S5. For most samples, CAM and MAM D_e values overlap within uncertainties, and ages were calculated using the CAM value, as it is less sensitive to outliers. The MAM was chosen when an overdispersion >10% was observed in combination with the presence of a skewed distribution of individual D_e values. This applied to 3 samples for IRSL and 10 for pIR (Supplementary Table S6).

Fading tests were carried out to assess the stability of the different luminescence signals using three previously measured aliquots of 10 representative samples. L_n/T_n was determined nine times for prompt measurements and for at least 11 different

storage times (between 1 h and 13 days). An average (central value) fading rate of $3.7 \pm 0.2\%$ per decade (normalized to 2 days) for IRSL was used to correct all final D_e values. Fading correction was carried out following Huntley and Lamothe (2001), using the R script by Kreutzer et al. (2020). For pIR, a fading rate of $0.94 \pm 0.45\%$ per decade (normalized to 2 days) was determined, which is considered to not require correction for fading for this signal (e.g., Thiel et al., 2011).

The concentration of dose rate–relevant elements (K, Th, U) was determined by neutron activation analyses by Bureau Veritas Laboratories, Canada (https://www.bvna.com). An *a*-value of 0.07 ± 0.02 was assumed. For all samples, water uptake capability was measured using the Enslin-Neff test (DIN 18132) from which the average sediment water content during burial was estimated considering the hydrological situation (presence of water table, etc.). Cosmic dose calculations follow Prescott and Hutton (1994), correcting for overburden and geographical position. Calculation of dose rates was carried out with ADELE v. 2017 software (https://add-ideas.com). The dosimetric data and ages are summarized in Supplementary Tables S4–S6.

Results

Dating results and interpretation

The chronological framework of the stratigraphic units and different paleochannels has been established by luminescence and radiocarbon dating. The ages of the sediments, which range from 22.0 ± 2.9 ka to 0.6 ± 0.1 ka, are presented within the context of the cores. Fifteen radiocarbon ages from peat and organic-rich sediments are listed in Table 1. With two exceptions, replicate radiocarbon measurements overlap within uncertainties, implying confidence in the dating results. However, some discrepancies in comparison to IRSL dating will be discussed later. For sample POZ-151145 (Artzenheim 1, depth 245 cm), one single age out

of seven ages for the same peat horizon is outside the uncertainty range of the other samples. For this sample, the laboratory reported a very low carbon content (0.4 mg C), which may explain the outlier. For the other outlier (POZ-151611, Daschsbrunnen, depth 105 cm) no such explanation is available.

For luminescence dating, the fading-corrected IRSL and pIR ages are presented in Figure 5. In particular, the plot of pIR/IRSL age ratio versus IRSL age (Fig. 5b) reveals that there is only a slight offset in age for samples >5 ka (average ratio = 1.09 ± 0.12), but that the offset varies greatly and is very large for some samples <5 ka. We interpret this observation to reflect the larger effect of incomplete resetting of the pIR signal in young samples, where a small residual dose will have a large effect on the calculated age. This comparison also implies that the applied fading correction of the IRSL signal does sufficiently account for signal loss due to anomalous fading, giving confidence in the IRSL age estimates and leading to the preferential use of these over the pIR ages in the discussion of the chronological framework.

### Descriptions of sediment cores

The stratigraphic logs of the investigated paleochannels and the natural levee of the Ill River are described in detail (see Supplementary Table S7 for geographic coordinates of the sediment cores). Descriptions are limited to the infill sediments, because the Pleistocene gravel (SU 1) ubiquitously forms the base of the cores (Figs. 6–9).

Baltzenheim

This sediment core was obtained from the Baltzenheim paleochannel, which is about 2 km west of the present-day Rhine (Fig. 1c). The infill sequence begins at 2.4 m below surface (bs) with beige medium sand with occasional pebbles, which progressively grades to silty fine sand up to 0.35 m bs (Fig. 6a). From 0.35

Table 1. Accelerator mass spectrometry (AMS) radiocarbon (with 2σ uncertainties) data for the samples from Artzenheim 1, Daschsbrunnen, and Spitzbrunnen paleochannels.

Lab code	Paleochannel	Depth (cm)	Material	^{14}C age (BP)	Calibrated ^{14}C age (cal BP)	Comment
POZ-151144	Artzenheim 1	220	Seed	5370 ± 35	6280–6010	0.6 mg C
POZ-151145	Artzenheim 1	245	Charcoal	3445 ± 35	3830–3580	0.4 mg C
POZ-151146	Artzenheim 1	260	Seed + charcoal	5615 ± 35	6490–6310	0.9 mg C
POZ-151148	Artzenheim 1	305	Seed	5605 ± 30	6450–6310	
POZ-151360	Artzenheim 1	305	Twig	5560 ± 35	6400–6300	
POZ-151149	Artzenheim 1	325	Seed	5610 ± 35	6480–6300	
POZ-151251	Artzenheim 1	340	Seed	5530 ± 30	6400–6290	
POZ-151113	Spitzbrunnen	80	Charcoal	160 ± 30	230–160	
POZ-151114	Spitzbrunnen	80	Charcoal	135 ± 30	180–170	
POZ-151252	Spitzbrunnen	120	Charcoal	610 ± 30	650–550	
POZ-151037	Spitzbrunnen	120	Seed	575 ± 30	640–530	
POZ-151396	Daschsbrunnen	95	Twig	1255 ± 30	1280–1070	
POZ- 151359	Daschsbrunnen	95	Wood	1370 ± 30	1350–1180	
POZ-151038	Daschsbrunnen	105	Leaf	1180 ± 30	1180–980	
POZ-151611	Daschsbrunnen	105	Wood	130 ± 30	200–190	
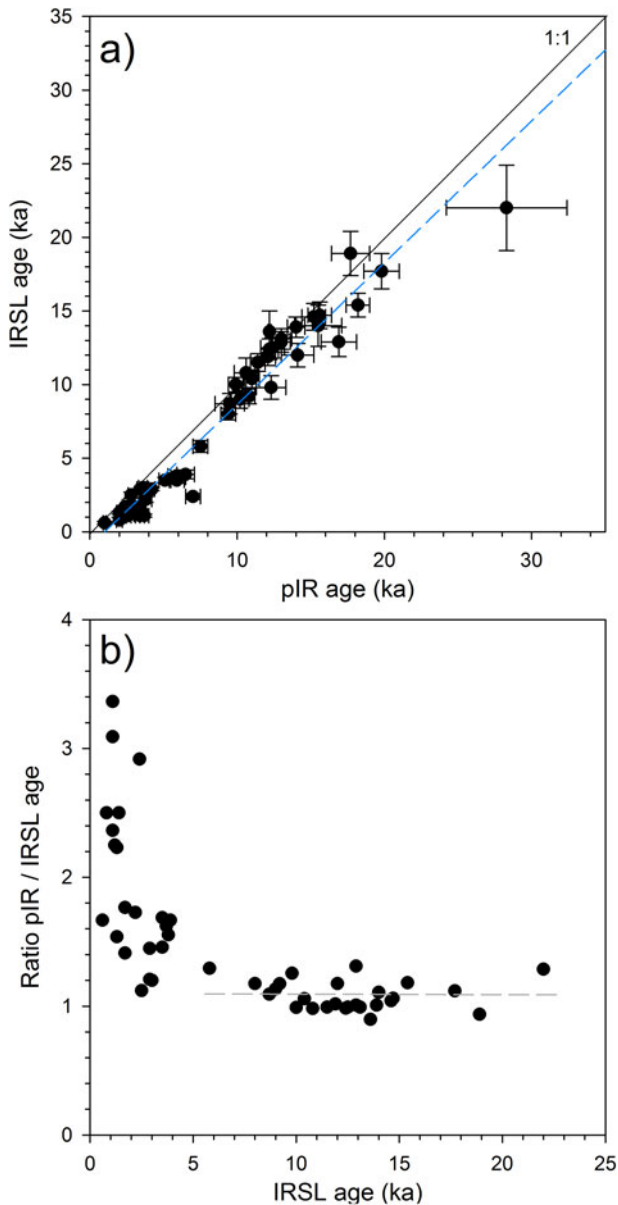
Figure 5. Comparison of fading-corrected infrared stimulated luminescence (IRSL) and post-IR (pIR) ages. (**a**) Direct plot of IRSL versus pIR and (**b**) plot of IRSL age versus the ratio pIR/IRSL age.

to 0.20 m bs, another unit of medium sand interrupts the fining upward sequence, which is subsequently overlaid by a layer of dark-brown silty loam. Except for a few peaks, all the sediment units show low OM values but relatively high carbonate content (ca. 20%). IRSL screening reveals a single accumulation phase for the channel fills, with L_n/T_n values ranging from 0.1 to 0.4, but with outliers at 2.4 and 2.1 m bs, IRSL dating places the accumulation phase of the sandy units between 3.7 ± 0.2 and 3.5 ± 0.2 ka. According to the MIRS provenance data, this paleochannel's infills are totally attributable to the Rhine River catchment.

Artzenheim 1a
This core is the first of two sediment cores taken from the Artzenheim 1 paleochannel, located around 2.5 km west of the current Rhine (Fig. 1c). The lowermost part of the core, between

4.8 and 3.8 m bs, consists of beige medium sand with very low OM and carbonate content (Fig. 6b). This unit is overlain by brownish-gray silty fine sand (3.8–3.4 m bs) with higher OM content (ca. 10%) and a sharp increase in carbonate content (>30%). Clastic sediment deposition ceases at 3.4 m bs, with the accumulation of a 1.7-m-thick sequence of peat and peaty mud containing abundant plant macro-remains. This peat sequence is interbedded with thin carbonate layers (carbonate concretions and shell fragments) with very high carbonate concentrations (up to 70%). The basal sandy deposits are IRSL dated to 9.0 ± 0.6 and 9.8 ± 0.8 ka, respectively, while AMS radiocarbon dates for the overlying organic sediments (peat and gyttja) range from 6490 to 6010 cal BP (Fig. 6b, Table 1).

From 1.65 m bs, clastic fluvial deposition continues, first with gray clayey silt and then with beige silty sand (1.22–1.02 m bs). This is followed by brown clayey silt, which is topped by dark-brown silty loam. Overall, the L_n/T_n values of the channel fills decrease toward the top, ranging from 0.8 to 0.05, with some dispersion between 2.3 and 2.31 m bs. IRSL dating yielded an age of 2.5 ± 0.2 ka for the gray clayey silt and 0.6 ± 0.1 ka for the brown clayey silt. This paleochannel's sedimentary units all have a distinct Rhine provenance semblance.
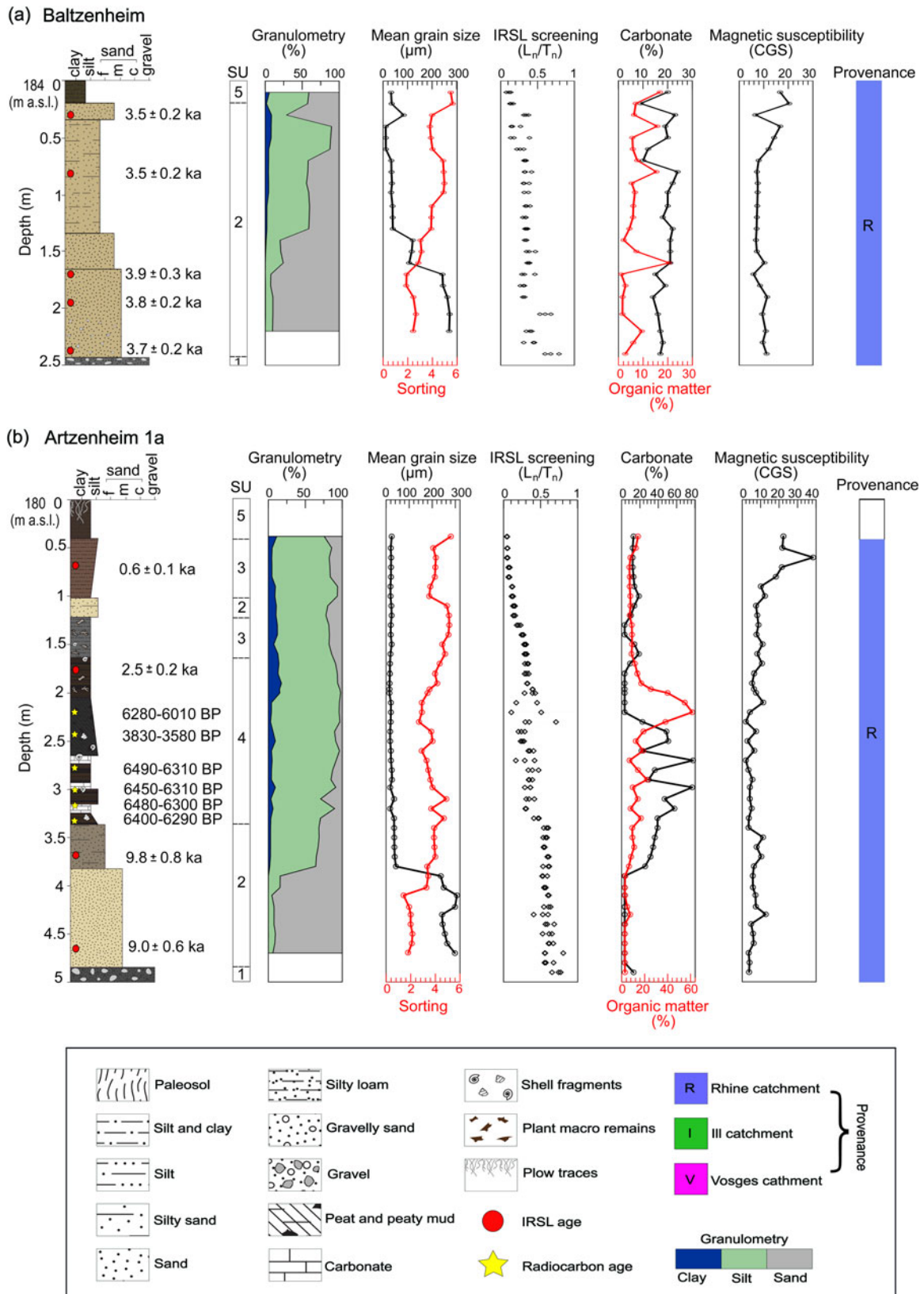
Artzenheim 1b
This is the second sediment core from the Artzenheim 1 paleochannel. The 2-m-long core is mainly made up of beige fine to medium sand that grades into silty fine sand (Fig. 7a). These sandy channel fills have a relatively high carbonate content (>25%), whereas OM values are generally very low (<3%). The basal part of the sand units is dated to 8.0 ± 0.4 ka, while the upper silty sand layer yielded an IRSL age of 12.9 ± 1.0 ka. From 0.55 to 0.35 m bs, the sediments change to a thin clayey silt unit of comparable geochemical composition. The depositional age of this unit is 5.8 ± 0.4 ka. Brown silty loam makes up the uppermost 0.35 m of the core. OM levels are considerably higher than in the clayey silt, but the carbonate content is reduced to <15%. The L_n/T_n values of the channel fills average 0.7 between 1.8 and 0.6 m bs, with two values at 0.4 and 0.5 m bs recording an average of 0.5. Above 0.4 m bs, the L_n/T_n reveals very low values of around 0.07. All the sedimentary units here, like those in the Baltzenheim and Artzenheim 1a, are from the Rhine catchment.

Artzenheim 2
This 3-m-long sediment core was obtained from the Artzenheim 2 paleochannel, about 5 km west of the current Rhine (Fig. 1c). The lower part of the core, from 2.7 to 1.5 m bs, is composed of gray medium sand with some pebbles interspersed with two silty sand intervals. Except for a carbonate peak at 1.9 m bs, these sandy channel deposits have very low carbonate (ca. 2%) and OM content (1%). From 2.7 to 0.7 m bs, the channel fills have an average L_n/T_n value of around 1, but values above 0.7 m bs decrease steadily from 0.5 to 0.1. IRSL dating returned an age of 12.5 ± 0.7 for the lowermost part of the medium sand. From 1.5 to 1.3 m bs, there is a fining upward from medium sand to silty fine sand, with a corresponding increase in carbonate content (ca. 10%) and OM content (ca. 8%). The overlying sediment layer up to 0.7 m bs consists of dark-brown organic-rich clayey silt with a thin lens of silty fine sand (ca. 10 cm thick). This change in deposits is also accompanied by an increase in OM content while maintaining a very low carbonate content. The thin silty sand layer is dated to 14.0 ± 1.4 ka, whereas the

Figure 6. Stratigraphic logs of the (**a**) Baltzenheim and (**b**) Artzenheim 1a paleochannels (see Fig. 1c for paleochannel locations), illustrating facies association, chronological information, granulometry, sedimentological and geochemical data, and provenance of various sediment units.
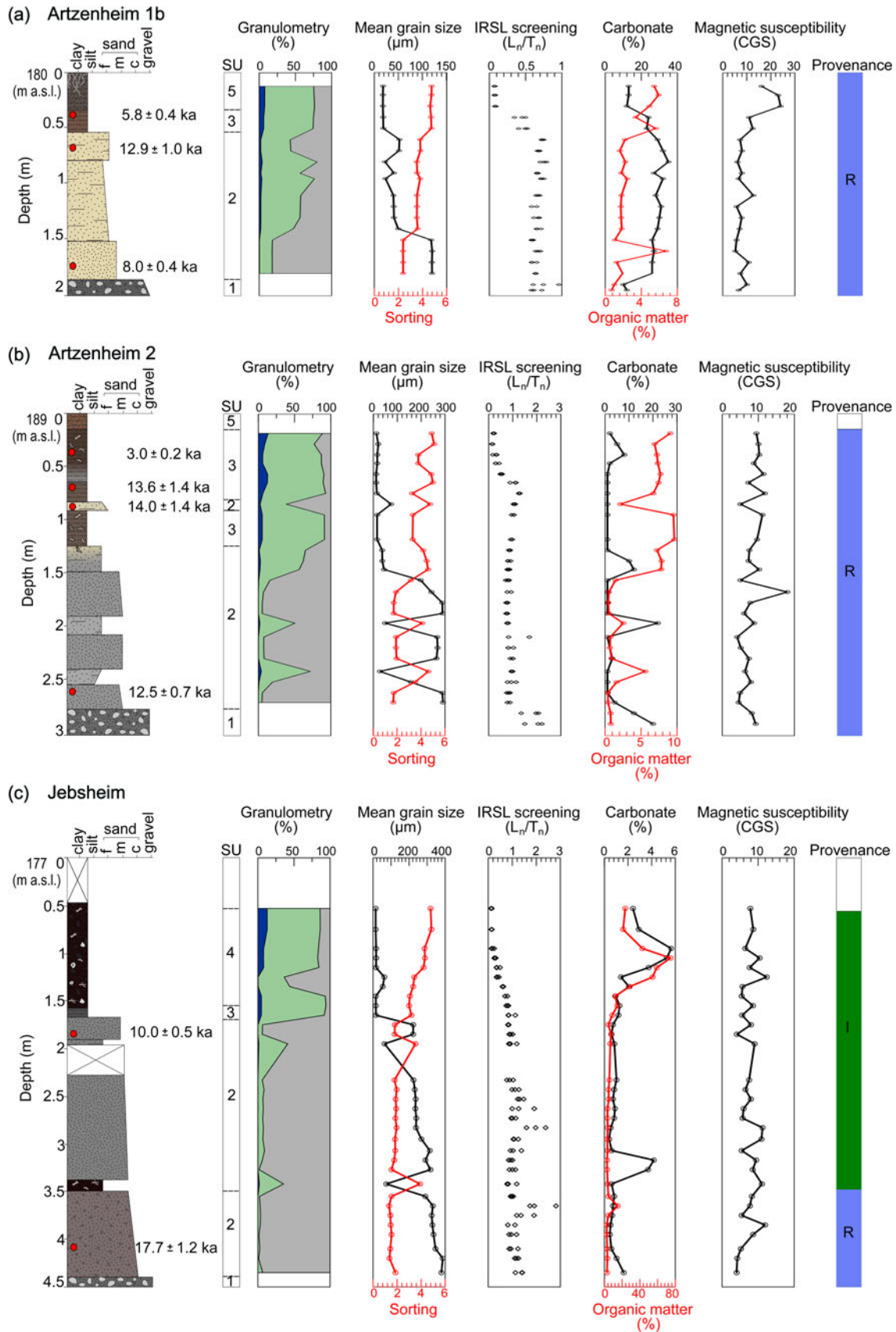
Figure 7. Stratigraphic logs of the (**a**) Artzenheim 1b, (**b**) Artzenheim 2, and (**c**) Jebsheim paleochannels (see Fig. 1c for paleochannel locations), illustrating facies association, chronological information, granulometry, sedimentological and geochemical data, and provenance of various sediment units. See Fig. 6 for the legend.

overlying clayey silt shows an age of 13.6 ± 1.4 ka. A light-gray to brown clayey silt (0.5 m thick) with a depositional age of 3.0 ± 0.2 ka overlies the clayey silt, while the top 0.2 m of the core is composed of brown silty loam. All infill sediments of this paleochannel show a Rhine provenance.

Jebsheim

The sediment core from this paleochannel is 4.5 m long, with the lowermost part (4.4–3.5 m bs) composed of reddish-gray gravelly sand (Fig. 7c). Above this unit is a thin layer (~15 cm) of dark-brown, silty, fine sand containing partially disintegrated plant pieces. The next sediment layer up to 1.7 m bs consists of gray medium sand with an upper increase of fine sand. The sands are overlain by a thin layer of dark-gray clayey silt. Carbonate and OM content are very low for these units, except for the silty fine sand, which has rather relatively high OM values (ca. 15%). From the base of the channel to 1.7 m bs, the channel fills exhibit an average L_n/T_n value of 1.1, with considerably higher values recorded at 3.7 and 2.8 m bs. According to the IRSL age obtained at a depth of 4.1 m bs, the gravelly sand has a deposition age of 17.7 ± 1.2 ka. In contrast, the overlying medium sand unit is IRSL age dated to 10.0 ± 0.5 ka. A dark-brown peat layer interspersed with layers of peaty mud (between 1.6 and 0.5 m bs) overlies the sandy channel deposits. The peat has naturally high levels of OM (up to ~75%) and a relative increase in carbonate content in its upper part due mainly to shell fragments. Between 1.7 and 0.5 m bs, the peat layer shows L_n/T_n values that decline steadily from 0.7 to 0.05. Sediments from 0.5 m bs to the surface were not recovered due to sediment loss during coring. However, the cross-sectional profile of this paleochannel reveals that the peat layer extends to about 0.3 m depth and is followed by an organic-rich, dark-brown clayey silt (Supplementary Fig. S1). According to the MIRS data, the basal gravelly sand is Rhine sourced. The overlying units, silty sand, medium sand, clayey silt, and peat, on the other hand, are consistent with an Ill provenance source.

Blind

The basal part of the Blind sediment core (1.94–1.52 m bs) consists of gray gravelly sand with a depositional age of 22.0 ± 2.9 ka (Fig. 8a). This unit is topped by light-gray fine to medium sand between 1.52 and 1.28 m bs. From a depth of 1.28 to 0.97 m bs, sediment is missing in the core. However, the cross-sectional profile of the paleochannel reveals that the sand deposit extends to a depth of 0.97 m bs (Supplementary Fig. S1). IRSL dating reveals an age of 12.0 ± 0.8 ka (depth of 1.3 m) for the medium sand unit. Very low OM values but moderate carbonate content (up to 15%) characterizes these sandy deposits. The overlying strata comprises a brown clayey silt unit (ca. 1 m thick) that gradually transitions to an organic-rich clayey-silt unit that caps the sequence. These upper sediment units are distinguished by elevated values of OM but relatively low carbonate content. IRSL dating gives an age of 1.7 ± 0.1 ka for the lowermost part of the clayey silt and 1.3 ± 0.1 ka for its upper reaches. The L_n/T_n values in the lower half of the channel, from the base to 1.3 m bs, decrease steadily from 1.6 to 1, whereas values above 0.9 m bs are significantly lower, averaging 0.2. The basal gravelly sand unit has a Rhine origin, whereas the medium sand and clayey silt units are Ill derived.

Riedbrunnen

The basal part of this core (1.68–1.33 m bs) is made up of beige fine sand, which grades upward into silty sand between 1.33 and 0.85 m bs (Fig. 8b). OM values within these units are very low (<4%), whereas carbonate content averages around 15%. This unit is followed by a succession of light-gray clayey silt (0.85–0.42 m bs) with elevated carbonate content (>50%) but with low OM values. From the base of the fine sand unit to the middle of the clayey silt (1.68–0.7 m bs), the average L_n/T_n value of the channel fills is approximately 1. In contrast, values above 0.7 m bs are considerably lower and decrease steadily from 0.3 to 0.1. The IRSL dating shows an age of 12.4 ± 0.7 ka for the fine sand unit and 11.9 ± 0.6 ka at the top of the silty sand layer. The lower portion of the clayey silt (0.85–0.62 m bs) is dated to 18.9 ± 1.5 ka, while its upper part (0.62–0.42 m bs) has a depositional age of 8.7 ± 0.7 ka. The uppermost 0.4 m of the core consists of organic-rich silty loam with partially decayed plant macro-remains. This unit shows extremely low carbonate (ca. 1%) and high OM values (20–30%). Except for the uppermost unit (silty loam), all sedimentary units in the Riedbrunnen paleochannel have a Rhine provenance (Fig. 8b).

Orchbach

The Orchbach paleochannel is approximately 350 m east of the Ill River, sometimes closer (Fig. 1c). The 3-m-long sediment core recovered from this paleochannel comprises gray medium sand in its lowest section (2.85–2.55 m bs; Fig. 8c). A dark-brown organic-rich sandy silt (0.2 m thick) separates this basal sand from another gray medium sand from 2.34 to 1.87 m bs. Between 1.87 and 1.65 m bs, another layer of silty sand overlies this unit. Except for the organic-rich sandy silt, which has a moderate OM content (ca. 10%), all of these sandy channel fills have extremely low OM and carbonate concentrations. IRSL screening shows an average L_n/T_n value of 1.1 for these sandy units. The lower sand unit is dated to 12.9 ± 0.7 ka, while the upper sand unit has IRSL ages of 13.1 ± 0.7 ka at its base and 11.5 ± 0.6 ka at its top.

The sandy channel fills are overlain by a gray clayey silt unit (1.65–0.84 m bs) that progressively grades into brown clayey silt (0.84–0.25 m bs) containing a few shell fragments and plant macro-remains. Within these units, OM values are comparatively high (ca. 10–15%), although carbonate levels remain very low. The gray clayey silt unit shows decreasing-depth L_n/T_n values ranging from 0.3 to 0.9, whereas the brown clayey silt has more uniform values averaging 0.2. The IRSL dating yielded an age of 10.8 ± 1.0 ka for the lowest part of the gray clayey silt. In comparison, the upper portion of the brown clayey silt is dated to 1.4 ± 0.1 ka (Fig. 8c). The uppermost 0.25 m of the core is formed of dark-brown clayey silt with some sand. According to MIRS provenance data, all the sediment units of the Orchbach paleochannel are primarily attributed to the Ill catchment.

Levee

This sediment core was collected on the Ill River's natural levee (Fig. 1c). The sedimentary sequence begins with a gray medium sand grading to silty fine sand from 2.0 to 1.76 m bs (Fig. 9a). This is followed by a beige-to-brown clayey silt layer between 2.0 and 1.76 m bs and a silty sand layer between 0.71 and 0.57 m bs. The OM values for these units gradually increase (2–8%), but carbonate concentrations have low values. The medium sand and clayey silt units are IRSL dated to 2.9 ± 0.1 ka and 2.2 ± 0.2 ka, respectively, while the silty sand has a depositional age of
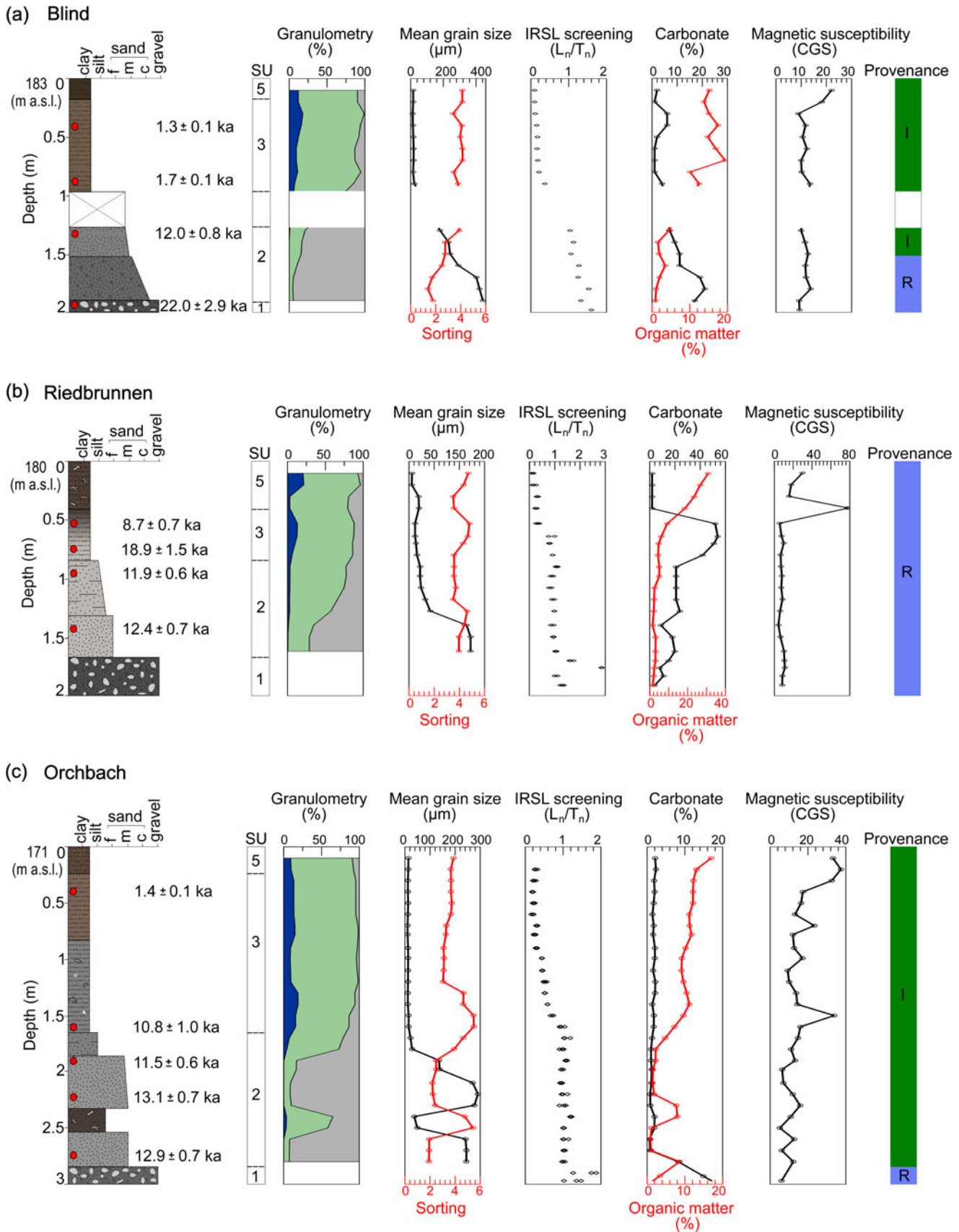
Figure 8. Stratigraphic logs of the (**a**) Blind, (**b**) Riedbrunnen, and (**c**) Orchbach paleochannels (see Fig. 1c for paleochannel locations), illustrating facies association, chronological information, granulometry, sedimentological and geochemical data, and provenance of various sediment units. See Fig. 6 for the legend.

1.1 ± 0.1 ka. From 0.57 to 0.32 m bs, a break in sedimentation reveals the development of a reddish-brown paleosol. The paleosol horizon is characterized by a crumbly structure with granular peds and clay illuviation. From 0.32 m bs to the surface, sedimentation proceeds with the deposition of a silty sand unit that grades to fine sand containing abundant plant macro-remains. This unit is IRSL dated to 1.1 ± 0.1 ka. IRSL screening indicates low L_n/T_n values ranging from 0.1 to 0.4 for the levee's sedimentary sequence, with outliers at 2.10 and 2.40 m bs. All sediment units in this core show an Ill provenance.

Wurzelbrunnen

This Wurzelbrunnen paleochannel is located around 450 m to the west of the Ill River (Fig. 1c). The infill sequence of this 2-m-long sediment core begins with a gray medium to coarse sand unit between 1.81 and 1.50 m bs. This basal sand is separated from a gray medium sand unit between 1.36 and 1.11 m bs by a 0.14-m-thick layer of gravelly sand. Between 1.11 and 1.03 m bs, another layer of gravelly sand lies above this unit. The gravelly sand is covered by a layer of fine, light-gray silty sand (1.03–0.80 m bs). Except for the fine silty sand, which is carbonate-free, all sandy channel fills have significant carbonate concentrations (15–20%) but extremely low OM content (ca. 1–2%). IRSL screening reveals two distinct depositional periods for this paleochannel. A first phase between 1.81 and 1.03 m bs with average L_n/T_n values of 1.2 and a few outliers, followed by a second phase between 1.03 and 0 m bs with average values of 0.25. The lower coarse sand unit is IRSL dated to 14.7 ± 0.9 ka, while the upper gravelly sand unit has a depositional age of 13.9 ± 0.7 ka. In comparison, the silty sand is dated to 1.7 ± 0.1 ka (Fig. 9b). A brown–dark brown clayey silt unit that extends from 0.80 m bs to the surface overlies the sandy channel fills. Within this unit, OM values are relatively high (around 10–15%), while carbonate levels remain very low (ca. 1%). IRSL dates this unit to 2.4 ± 0.2 ka. MIRS analysis indicates that the coarse and gravelly sand units are formed of Rhine-derived sediments. The silty sand and clayey silt units, in contrast, are primarily associated with the Ill River.

Daschsbrunnen

The Daschsbrunnen paleochannel is also situated west of the Ill River, about 1 km from the present Ill River channel (Fig. 1c). This paleochannel's sediment core is 2 m long, with the lowermost part (1.65–1.33 m bs) composed of gray fine sand with scattered pebbles, grading to medium sand between 1.33 and 1.12 m bs (Fig. 9c). Following this is a 0.2-m-thick layer of gray silty sand with plant macro-remains. These units have very low OM and carbonate concentrations, except for the basal fine sand unit, which has a moderate carbonate content (ca. 10%). IRSL screening indicates two depositional phases for this paleochannel, similar to the Wurzelbrunnen paleochannel. An initial phase with average L_n/T_n values of 1.2 between 1.65 and 1.12 m bs, and a second phase with average values of 0.2 between 1.12 and 0.2 m bs. The fine sand has a depositional age of 14.6 ± 0.9 ka, according to IRSL data, while the overlying medium sand unit has an IRSL age of 10.4 ± 0.6 ka. Radiocarbon ages for the lower and upper parts of the silty sand date the unit to 1350 to 980 cal BP (Fig. 9c, Table 1). The overlying sediment unit is grayish-brown clayey silt from 0.89 to 0.20 m bs, while the uppermost part of the core, between 0.2 m bs and the surface, is dark-brown loamy silt. These units also have very low carbonate concentrations but relatively higher OM values. IRSL dating of the bottom and

upper portions of the clayey silt places the age of the unit between 2.9 ± 0.2 ka and 1.2 ± 0.1 ka. The MIRS data show that the basal sandy channel infills have a Rhine origin, while the silty sand and clayey silt units show an Ill signature (Fig. 9c).

Spitzbrunnen

The Spitzbrunnen paleochannel is located around 2.2 km east of the Fecht River and 1.9 km west of the Ill River and is the most westerly of the investigated paleochannels (Fig. 1c). The sediment infill begins with dark-gray gravelly sand (1.92–1.64 m bs) that progresses to gray medium sand from 1.64 to 1.31 m bs (Fig. 9d). These units show very low OM values and are mainly carbonate-free, while the average L_n/T_n value is 1.5. IRSL dates the gravelly sand to 15.4 ± 0.8 ka, whereas the medium sand dates to 9.2 ± 0.5 ka. The next sediment layer up to 1.15 m bs comprises dark-gray silt with abundant plant macro-remains. According to two radiocarbon ages obtained at 1.2 m bs, the deposition of this unit was between 530 and 650 cal BP (Fig. 9d, Table 1). The next layer is a light-gray clayey silt between 1.15 and 0.75 m bs, which changes to brownish-gray clayey silt at 0.75 m and continues to the surface. Very low carbonate levels characterize these silty units but comparatively higher OM values (ca. 10%). From the base of the dark-gray silt to the top of the brownish-gray clayey silt, the L_n/T_n values decrease progressively from 0.7 to 0.1, with a few scatters recorded at 1.21 and 0.34 m bs. Two radiocarbon ages obtained at 0.90 m bs date the light-gray clayey silt unit between 160 to 230 cal BP (Fig. 9d, Table 1), whereas IRSL dating at 0.85 m bs yielded an age of 1.3 ± 0.1 ka for this unit (Fig. 9d, Supplementary Table S6).

A comparable depositional age of 1.1 ± 0.1 ka is recorded for the overlying grayish-brown clayey silt. According to the MIRS data, the basal gravel unit has a Rhine origin; the sand units are predominantly from the Vosges source area, whereas the overlying silty units originate from the Ill catchment (Fig. 9d).

Discussion

Dating inconsistencies

The radiocarbon ages from the Daschsbrunnen and Spitzbrunnen paleochannels of 1350 to 160 cal BP (Fig. 9c and d, Table 1) are not in stratigraphic order and younger than the IRSL-dated stratigraphic units above them (Fig. 9c and d). These discrepancies suggest that either the radiocarbon ages are underestimating or the IRSL ages are overestimating. However, radiocarbon ages reported for comparable stratigraphic units from neighboring paleochannels (Al Siddik, 1986; Al Siddik et al., 1989) are consistent with our IRSL ages and fall within the same age interval. Hence, we consider the radiocarbon ages obtained from the Daschsbrunnen and Spitzbrunnen paleochannels too young (underestimated). These anomalously young radiocarbon ages are most likely due to contamination with younger carbon during the sampling or preparation process. Therefore, the radiocarbon ages obtained from the Daschsbrunnen and Spitzbrunnen paleochannels are disregarded for subsequent interpretations.

The reported IRSL ages are generally consistent and in stratigraphic order, except for two samples: Az1b-70 cm (Artzenheim 1b, depth 70 cm) and Ried 70 cm (Riedbrunnen, depth 70 cm). These ages are much older than those of the stratigraphic units below them (Figs. 7a and 8b, Supplementary Table S6). Considering their stratigraphic placement, the ages of samples Az1b-70 cm (12.9 ± 1.0 ka) and Ried-70 cm (11.9 ± 0.6 ka) seem
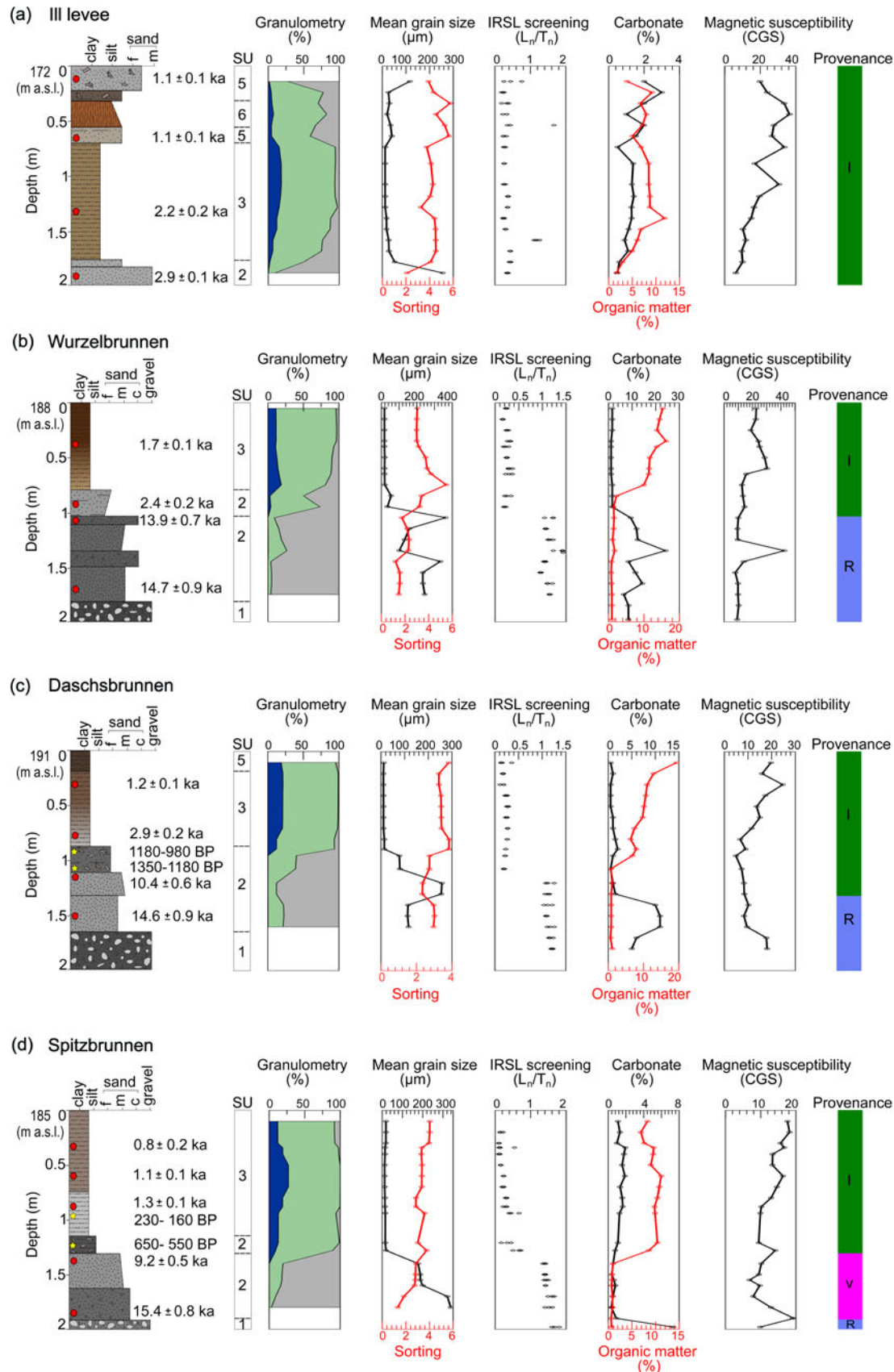
Figure 9. Stratigraphic logs of (**a**) the Ill levee and (**b**) Wurzelbrunnen, (**c**) Daschsbrunnen, and (**d**) Spitzbrunnen paleochannels (see Fig. 1c for levee and paleochannel locations), illustrating facies association, chronological information, granulometry, sedimentological and geochemical data, and provenance of various sediment units. See Fig. 6 for the legend.

largely overestimated. This is likely due to older sediments being reworked and redeposited in the paleochannels. During high flood events, sediments from proximal Hardt Grise areas (reworked Pleistocene terrace of the Rhine; Fig. 3) could have been eroded and redeposited in paleochannels. The sediments would only have been transported over a short distance and therefore would likely have been only very briefly exposed to daylight, resulting in higher age estimates than expected. Calcareous sediments from the Hardt Grise have also been documented in some Holocene paleochannels south of Illhaeusern (Al Siddik, 1986; Al Siddik et al., 1989). This is consistent with the occurrence of older Hardt Grise sediments in Artzenheim 1b, which is located very close to a Hardt Grise area. Similar sediments are also found in the Riedbrunnen paleochannel, located downstream of the Hardt Grise area, southwest of Bischwihr (Figs. 3 and 4; Hirth, 1971). Moreover, sediment input from the Hardt Grise explains the high carbonate content and unexpected Rhine provenance of the upper sediment successions of the Riedbrunnen paleochannel (Fig. 8b) despite its remoteness from the Rhine (Fig. 4).

Facies assignment

The sedimentary deposits in the investigated paleochannels and levee are classified into six lithogenetic units (SU 1 to SU 6). Except for the paleosol (SU 6), these units have been previously described by Abdulkarim et al. (2022) based mainly on hand-augured core data. However, the present study additionally integrates sedimentological, geochemical, and geochronological data to highlight unit characteristics further and validate the groupings. The lithogenetic units represent distinct energy conditions, sediment transport and deposition processes, and different phases of channel activity. Thus, identifying these units and establishing their provenance and ages enables reconstruction of past fluvial activity in the area.

SU 1 consists of cobble-rich gravelly sediments found at the base of the paleochannels. It differs from units above due to larger particle sizes, gravel predominance, and poorly sorted sediments (Figs. 6–9), suggesting formation through nonselective bedload transport under high-energy depositional conditions (e.g., Chardon et al., 2021). These gravel deposits show an unambiguous Rhine origin (from MIRS analysis), often with high carbonate content and minimal OM. Interpreted as Pleistocene Rhine gravel, SU 1, while not constituting the direct infill of the paleochannels, may be geomorphologically reworked and deposited within them, providing crucial insights into channel dynamics.

SU 2 is composed of sands, gravelly sands, and silty sands in a fining upward sequence with moderate to poor sorting (Figs. 6–9). These sandy successions, featuring gravelly channel lags and sandy channel infills, indicate deposition at the onset of infill during moderate- to high-energy flow episodes (e.g., Plotzki et al., 2015; Delile et al., 2016). The SU 2 deposits are found at varied depths and range in age from the late glacial to the Late Holocene. Furthermore, they bear Rhine, Ill, and Vosges provenance signatures. Thus, SU 2 units give evidence of channel activity and deposition during a permanent or irregular connection to the different river systems in the region.

SU 3 generally consists of fine-grained silty and clayey sediments, occasionally with thin layers of very fine sand. These well-sorted sediments have higher OM content than SU 2 and contain shell fragments and plant macro-remains (Figs. 6–9). The sedimentary characteristics and stratigraphic position of these deposits imply deposition in low- to very low energy depositional environments. Furthermore, their transport and deposition underline mostly homogenous suspension (e.g., Delile et al., 2016), which could indicate channels with no (or only a limited) upstream hydrological link to a basin-fed river. The SU 3 deposits are mainly found directly above SU 2 deposits and span in age from the late glacial to the Late Holocene, also with different provenance sources. Thus, SU 3 sediments serve as key stratigraphic indicators for identifying phases of decreased fluvial activity and partial disconnection from feeding rivers (upstream).

Lithogenetic unit **SU 4**, found exclusively in the Artzenheim 1 and Jebsheim paleochannels (Fig. 6b and 7c), consists of dark-brown to black peat and peaty mud rich in OM, with abundant plant macro-remains. Some sections contain shell fragments and very thin, intermittent clastics (coarse sand and pebbles). In the Artzenheim 1 paleochannel, thin carbonate layers interlace with peaty mud, distinguished by extremely high carbonate concentration, low OM content, and the absence of plant macro-remains (Fig. 6b). The unit's sedimentary characteristics indicate autochthonous sedimentation with limited clastic deposition in settings of very low flow energy or stagnant water. Thus, the SU 4 lithogenetic unit marks a period of slowed or ceased fluvial activity in the Mid Holocene.

SU 5 comprises young surficial deposits (Subatlantic to Recent) that typically cap older units. These sediments, composed of clayey silt to silty loam with reworked sands, share similarities with SU 3 but differ in stratigraphy and genesis. SU 5 is formed through overbank deposition and is characterized by its darker colors, higher OM content, and fragmented plant macro-remains (Figs. 6–9). In addition, plowing traces and pedogenetic processes are frequently observed in the upper sections. The SU 5 lithogenetic unit indicates near-total channel abandonment, very low sedimentation rates, and nearly stable surface conditions.

SU 6 is limited to the natural levee of the Ill River, where it reaches a thickness of 25 cm (Fig. 8a). This unit, which represents a paleosol horizon, is distinguished by its distinctive rusty-brown color, lack of apparent laminations, and crumbly structure with granular peds and clay illuviation. This horizon lies between SU 5 units dated to the Late Holocene (1.1 ± 0.1 ka), indicating a short period of geomorphic stability and soil formation near the current Ill River channel during the Late Holocene.

Temporal trajectory of the fluvial hydrosystems

The data from this study and additional data from earlier studies (Hirth, 1971; Al Siddik, 1986; Boës et al., 2007; Schmitt et al., 2016; Chapkanski et al., 2020; Abdulkarim et al., 2022) were combined to reconstruct the late glacial and Holocene temporal trajectories of the fluvial hydrosystems in this section of the Upper Rhine alluvial plain, in response to different potential driving factors.

Late glacial (Oldest Dryas, Bølling-Allerød, Younger Dryas)

Channel activity during the Oldest Dryas stade is indicated by the coarse-grained channel fills of the Artzenheim 2 (PG 1), Jebsheim (PG 2), Blind (PG 3), Riedbrunnen (PG 3), Wurzelbrunnen (PG 3), Daschsbrunnen (PG 3), and Spitzbrunnen (PG 5) paleochannels. These deposits reflect rapid sedimentation (based on IRSL screening and IRSL dating data; Figs. 6–9, Supplementary Table S6) in a high-energy flow and depositional environment exclusively reflecting Rhine provenance. Based on the character of these deposits and the spatial distribution of the paleochannels,
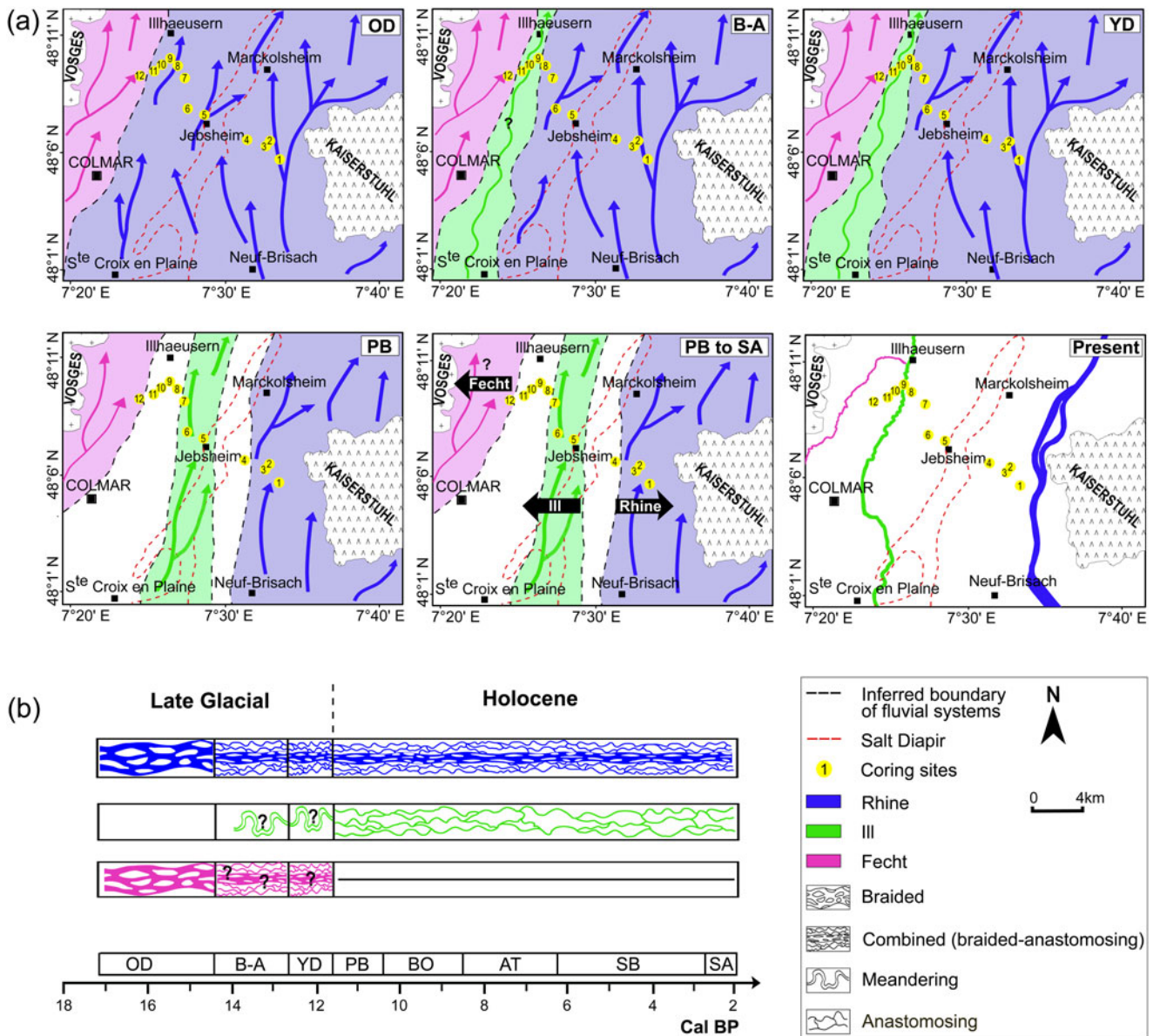
Figure 10. (**a**) Schematic reconstruction of the late glacial and Holocene fluvial temporal trajectory of the Rhine, Ill, and Fecht River systems in the study area. (**b**) A synthesis of changes in fluvial channel pattern during the late glacial and Holocene. Subdivision of late glacial and Holocene climatic periods according to Ivy-Ochs et al. (2004), Schirmer et al. (2005), Bos et al. (2008), and Kock et al. (2009). Abbreviations: OD, Older Dryas; B-A, Bølling-Allerød; YD, Younger Dryas; PB, Preboreal; BO, Boreal; AT, Atlantic; SB, Subboreal; SA, Subatlantic.

a braided Rhine system occupied nearly the entire alluvial plain during the Oldest Dryas (Fig. 10). This period was generally cold and arid, with reduced vegetation cover, much greater flow during floods, and high bedload (Kolstrup, 1980; Vogt, 1992; Mol et al., 2000). Moreover, during this period, a braided pattern was characteristic for other parts of the Upper Rhine River (Lang et al., 2003; Erkens et al., 2009; Lämmermann-Barthel et al., 2009) and was dominant in many other fluvial systems in northwestern and central Europe (Vandenberghe et al., 1994; Huisink 1997; Mol et al., 2000; Antoine et al., 2003; Kasse et al., 2005, 2010; Gao et al., 2007).

However, sediments in the Spitzbrunnen paleochannel (PG 5) dating to the Oldest Dryas show a strong Vosges catchment provenance (Fig. 9d), indicating that the Fecht River, or a precursor Fecht system, evolved independent dynamics during this period.

In addition, Hirth (1971) and Abdulkarim et al. (2022) identified parallels in the morphologic characters of the Spitzbrunnen paleochannel and the contemporary Fecht channel. The channel pattern of the Fecht during this period is undetermined. However, based on the coarse-grained nature of the Spitzbrunnen sediments, the prevailing climatic and environmental conditions, and the potential high bedload supply by the Fecht basin during this period, we assume a braided system, albeit a smaller one compared with the Rhine.

The transition from the Oldest Dryas to the Bølling-Allerød interstade is marked by the abandonment of braided Rhine channels, particularly in the western part of the plain (e.g., Daschsbrunnen and Wurzelbrunnen; PG 3), linked to the narrowing and eastward migration of the Rhine's active belt (Fig. 10). According to Dambeck and Thiemeyer (2002), the

northern Upper Rhine River evolved a meandering pattern during the Allerød, while Mäckel (1998) suggests that the entire Upper Rhine River developed a meandering pattern at the onset of the late glacial. However, our findings indicate concurrent channel activity during the Bølling-Allerød, as evidenced by the Riedbrunnen (PG 3) and Artzenheim 2 (PG 1) paleochannels. Notably, the channel fills consist of finer-grained sands, indicating a relatively moderate-energy environment. Thus, we hypothesize that the Rhine was still a multichannel river in this section of the Upper Rhine plain during the Bølling-Allerød, but with a complex pattern combining braided close to the thalweg and anastomosing at the margin of the fluvial hydrosystem. Furthermore, anabranching channels (Nanson and Knighton, 1996) were probably also present between these two pattern types (Schmitt et al., 2016). Similar complex, multi-threaded fluvial patterns during the interstades have been documented for parts of the northern Upper Rhine (Erkens et al., 2009), the Meuse River (Vandenberghe et al., 1994; Huisink 1997, 1999; Kasse et al., 2005), the Niers-Rhine (Kasse et al., 2005), and the Warta River (Vandenberghe, 1995).

The narrowing of the Rhine braided belt and partial changes in channel planform is most likely related to the climatic warming of the Bølling-Allerød and the resulting increase in vegetation cover (Schneider, 2000; Kasse et al., 2010 and references therein; Hoek et al., 2017), lower discharge, and decreased sediment supply by the basin (Kasse et al., 2010 and references therein). Alpine glacier retreats during the Oldest Dryas and the subsequent formation of numerous Alpine lakes (Hinderer, 2001; Ivy-Ochs et al., 2004) have also strongly influenced these fluvial dynamics, as these lakes functions as natural sediment traps (Wessels, 1998; Hinderer, 2001).

The transition to the Bølling-Allerød interstade with the Rhine narrowing and migrating eastward also explains the emergence of an individualized Ill River system in the study area. This appears evident in the Orchbach paleochannel (PG 3), where sediments originating from the Ill catchment were deposited during the Bølling-Allerød interstade (Fig. 8c). Schmitt et al. (2016) considered that the Ill hydrosystem formed at the start of the Holocene, but our findings place this about 2000 years earlier. The diminution of Alpine glaciers together with the narrowing of the Rhine active band, which moved eastward, is believed to have prompted the individualization of the Ill River during the Bølling-Allerød. However, unlike the Rhine sediments, Ill sediments were only found in the Orchbach paleochannel (PG 3). Consequently, we deduce that the Ill River was probably mostly meandering-like during this time period, but the formation of an anastomosing pattern for the Ill River had probably already begun at this time, possibly due to the morphological inheritance of the former braided Rhine pattern.

In contrast to the Oldest Dryas stade and Bølling-Allerød interstade, the channel morphology and infill successions do not evidence significant changes in fluvial processes associated with the Younger Dryas stade in the Upper Rhine plain. The Rhine and Ill systems probably maintained their combined braided-anastomosing and meandering-like patterns, respectively. This trend toward channel pattern stability at the beginning of the Younger Dryas has been documented for the northern Upper Rhine (Dambeck and Thiemeyer, 2002; Bos et al., 2008; Erkens et al., 2009), as well as for other European rivers such as the Warta River (Vandenberghe et al., 1994; Vandenberghe, 1995), Bergstrassen-Neckar (Dambeck and Thiemeyer, 2002; Bos et al., 2008), middle Tisza (Kasse et al., 2010), Niers-Rhine (Kasse

et al., 2005), and Lower Scheldt (Meylemans et al., 2013). The lack of fluvial adjustments in response to the Younger Dryas climatic oscillation may be attributable to the buffering effect that the massive Rhine system had against climate change (Bos et al., 2008) and the preservation of forest cover during the Younger Dryas (Schneider, 2000; Bos et al., 2008). Furthermore, the inherent characteristics of the alluvial plain (e.g., its broad width of more than 15–20 km) may also explain, at least partly, the lack of major fluvial adjustment to climate change (Vayssière et al., 2019 and references therein).

Early to Mid-Holocene (Preboreal, Boreal, and Atlantic)
According to our findings and previous studies (e.g., Boës et al., 2007; Schmitt et al., 2016), the Rhine at the Early Holocene was restricted to the alluvial plain's central and eastern reaches (Fig. 10). The channel pattern combined a braided and anastomosing pattern (Schmitt et al., 2016). This pattern contrasts with those of the northern Upper Rhine (Dambeck and Thiemeyer, 2002; Bos et al., 2008; Erkens et al., 2009) and other European rivers (Vandenberghe et al., 1994; Huisink, 1999), which are understood to have developed large-scale, single-thread meandering patterns in the Early Holocene. The development of a meandering pattern in these European rivers is attributed mainly to the renewed climatic warming of the Early Holocene and the associated lower discharges, decreased sediment supply, increased vegetation cover, relative bank stabilization, and low valley gradient. Thus, the evolution of an anastomosing channel pattern in the studied reach of the Upper Rhine was probably influenced by factors other than Early Holocene climate warming and environmental changes.

Possible controlling factors in the studied reach include the important width of the alluvial plain, a relatively low valley gradient (0.8–0.6%) compared with the upstream section of the alluvial plain, relative tectonic subsidence compared with the upstream and downstream areas (Vogt, 1992), and a propensity for sedimentation by fine sediments on the floodplain (Hirth, 1971; Ollive et al., 2006; Schmitt et al., 2016). This Holocene aggradation was also caused by the upstream Holocene incision of the Rhine River (Lämmermann-Barthel et al., 2009; Schmitt et al., 2016). In addition to these factors, Rhine side channels probably reoccupied numerous relict channels of the late glacial braided system (as well as younger braided Rhine channels when the Rhine moved eastward), which may have favored the anastomosing channel pattern. Thus, it appears that the late glacial braided Rhine system gradually metamorphosed into a moderate-energy braided-anastomosing system in the Early Holocene through a complex interplay of both climatic and non-climatic mechanisms.

The transition to the Holocene was also accompanied by significant changes to the Ill fluvial hydrosystem. Our data show that the Ill channel at Orchbach was abandoned around the beginning of the Holocene. At the same time, Ill-derived channel fills were deposited in the Blind (PG 3) and Jebsheim (PG 2) paleochannels between 12.0 ± 0.8 and 10.0 ± 0.5 ka (Figs. 7c and 8a, Supplementary Table S6). These changes in dynamics point to an active channel (or some significant side channels of the Ill River) in the central part of the plain from the start of the Holocene. Moreover, previous studies (e.g., Boës et al., 2007; Schmitt et al., 2016; Chapkanski et al., 2020) have also documented Ill-derived channel fills dating to the Preboreal in some paleochannels in the central part of the alluvial plain. Accordingly, we contend that during the Early Holocene, as the active channel belt of the Rhine narrowed and shifted eastward,

a Holocene Ill system evolved in the central part of the plain, reoccupying some abandoned Rhine channels. The newly formed Ill River showed concurrent activity in multiple channels, indicating that it was probably larger than its predecessor. It also adapted its morphology from a meandering-like pattern to a well-defined, multi-threaded anastomosing system, influenced by alluvial plain–scale controlling factors comparable to those influencing the Rhine (Schmitt et al., 2016).

The Rhine and Ill Rivers maintained their patterns throughout the Preboreal, Boreal, and early Atlantic. In addition, the Rhine probably gradually moved eastward during this phase, while the Ill River moved westward (Hirth, 1971; Schmitt et al., 2016). In contrast, the second half of the Atlantic is characterized by a slow-down of fluvial dynamics, with very low lateral channel dynamics. This phase was most likely fostered by the period's climatic evolution (warming), which resulted in a densely forested alluvial plain (Dambeck and Thiemeyer, 2002; Lang et al., 2003; Bos et al., 2008). Thus, the late Atlantic is characterized by a general decline in clastic channel fills in most of the investigated paleochannels and contemporaneous deposition of peat and organic sediments in some Early Holocene paleochannels, for example, Artzenheim 1 (PG 1) and Jebsheim (PG 2) (Figs. 6b and 7c).

Peat accumulation in the Artzenheim 1 paleochannel (PG 1) dates to the late Atlantic (Fig. 6b, Table 1). By considering peat dating from several paleochannels near Illhaeusern (Al Siddik et al., 1989; Chapkanski et al., 2020), we bracket the interval of the major organic sedimentation (peat and peaty mud) between the early Subboreal and late Atlantic. This interval agrees well with the period of enhanced peat and organic sedimentation recorded in other areas of the Upper Rhine Valley (e.g., Schneider, 2000; Dambeck and Thiemeyer, 2002; Bos et al., 2008; Erkens et al., 2011). Although this phase was characterized by reduced fluvial dynamics, intermittent clastics (sand and some pebbles) within the peat indicate that there were episodic flooding events. Consequently, we propose the early Subboreal to late Atlantic was a period of generally low fluvial activity, punctuated by periodic flooding with increased energy in the channel.

In contrast to the Rhine and Ill Rivers, the Fecht River's post-Preboreal trajectory remains vague. Nonetheless, we assume that it moved westward after abandoning the Spitzbrunnen paleochannel during the Preboreal (Fig. 9d). The absence of Vosgian sediment infill to the east of the Spitzbrunnen paleochannel (PG 5) supports this presumption.

Mid- to Late Holocene (Subboreal and Subatlantic periods)

The onset of the Subboreal, marked by a generally colder climate and reduced vegetation cover (Schneider, 2000; Bos et al., 2008), is characterized by a consequent resumption of fluvial dynamics. This is evidenced by the deposition of clastic channel fills and the contemporaneous cessation of peat accumulation. During the Subboreal, the densely forested Upper Rhine plain transformed into a more open landscape, with a decrease in woodlands and an expansion of meadows as well as agricultural activities, the latter at scales of both the alluvial plain and the catchment (Schneider, 2000; Dambeck and Thiemeyer, 2002; Lang et al., 2003; Bos et al., 2008). In contrast to earlier periods, these environmental changes were not just caused by natural forces but also by the expanding human impact on the environment. Human activity (deforestation, agriculture, and pastoralism), which had begun in the southern Upper Rhine region during the Atlantic, increased significantly from the Subboreal to the Subatlantic over a part of the catchment (Schneider, 2000; Kalis

et al., 2003; Lang et al., 2003; Mäckel et al., 2009; Holzhauer et al., 2017). Both climate and human factors led to higher rates of soil erosion and increased runoff and sediment supply to the Rhine and Ill fluvial systems (Al Siddik et al., 1989; Schneider, 2000; Dambeck and Thiemeyer, 2002; Lang et al., 2003; Bos et al., 2008; Hoffman et al., 2008; Erkens et al., 2009).

Despite the intensification of anthropogenic use of the plain, there is no indication of a significant local anthropogenic impact on the channel patterns in the studied reach. The Rhine and Ill systems maintained their braided-anastomosing and anastomosing patterns, respectively, throughout the Subboreal and Subatlantic, until nineteenth-century engineering works significantly altered their natural channel patterns and dynamics (e.g., Eschbach et al., 2018). Both rivers continued moving laterally across the plain, leaving behind a network of abandoned channels mainly filled with fine clastic sediments. The Rhine River likely maintained a continuous eastward movement and is believed to have reached its current position during the Iron Age (Schmitt et al. 2016). The Ill River, on the other hand, continued westward, reoccupying some abandoned Rhine channels (e.g., Figs. 7c and 8a). Our data indicate that the Ill River reached its westernmost extent, between the Daschsbrunnen (PG 3) and Spitzbrunnen (PG 5) paleochannels, around 1.7 ka. It subsequently began to move eastward, reaching its current position around 1.1 ka. The Ill River's western movement may have been impeded by the higher elevation in the west produced by the alluvial fan of the Fecht system (Supplementary Fig. S2).

Factors and processes of river displacements

Along with the narrowing of the active channel belt of the Rhine since the late glacial, we infer lateral displacements and channel abandonment of the Rhine, Ill, and possibly the Fecht Rivers throughout the Holocene. The narrowing of the Rhine's braided channel belt primarily resulted from climatic and environmental changes during the late glacial and the onset of the Holocene. However, long-lived anastomosing systems are characterized by regular avulsion processes (Nanson and Knighton, 1996; Morozova and Smith, 1999; Makaske, 2001; Makaske et al., 2002). These processes have been recorded in various long-lived (Holocene) anastomosing systems, such as the lower Saskatchewan River (Morozova and Smith, 1999), upper Columbia River (Makaske et al., 2002), and the Rhine-Meuse delta (Stouthamer and Berendsen, 2007). Hence, we propose that the Holocene lateral movements of the fluvial hydrosystems in the Ried Central d'Alsace, especially those of the Ill River, are most likely related to avulsion processes. For the Rhine River (western part of the hydrosystem), such processes probably combined with the metamorphosis of braided channels to anastomosing channels when the Rhine hydrosystem moved eastward.

River avulsion is a relatively abrupt and major diversion of water flow from an established channel to a new or preexisting channel in the floodplain, eventually leading to the formation of a new channel belt (Nanson and Knighton, 1996; Morozova and Smith, 1999; Makaske, 2001; Slingerland and Smith, 2004; Valenza et al., 2020). This dynamic process is a major feature in aggrading floodplains and is driven by various factors, including channel belt aggradation and sediment accumulation, longitudinal river gradient changes, fluctuations in water discharge, and tectonic activity (Nanson and Knighton, 1996; Morozova and Smith, 1999; Mohrig et al., 2000; Makaske, 2001; Slingerland and Smith, 2004; Aslan et al., 2005). Depending on the driving

factors and characteristics of the floodplain, avulsion typically occurs in one of two ways: either by construction of new channels into the floodplain via splay-complex progradation (first-order avulsion) or by reoccupation of preexisting floodplain channels (second-order avulsion) (Nanson and Knighton, 1996; Makaske, 2001).

The evidence supporting avulsion processes in the studied reach is primarily derived from the LIDAR digital elevation map of the area and field observations. These observations reveal that the floodplain landscape is characterized by topographic lows corresponding to paleochannels and distinct topographic highs near the paleochannel margins (relative elevation between 0.3 to 1 m), interpreted as remnants of channel levees. In addition, levees are evident in the cross-sectional profiles of specific paleo-channels (Supplementary Figs. S1 and S2). This configuration of relatively high channel margin levees and partially filled paleo-channels is commonly indicative of an alluvial plain where avulsion is a dominant fluvial process (Mohrig et al., 2000; Slingerland and Smith, 2004; Han and Kim, 2022; Martin and Edmonds, 2022). Schmitt et al. (2016) also proposed that a network of levees around the Ried Noir was built by a series of avulsions that coincided with the Ill River's westward displacement during the Mid-Holocene. Moreover, the present-day eastward trajectory of the Ill River indicates a significant tendency to reoccupy the proximal Orchbach River through a characteristic second-order avulsion style. Accordingly, we propose that several cycles of avulsion occurred in the study area, and the avulsion dynamics were influenced by a combination of relatively high aggradation rates, the presence of paleochannels in the floodplain, and neotectonics (notably relative subsidence as well as local diapir uplift; Schumm et al., 2000).

The relatively high rate of general aggradation (sand levees and mud in other parts of the floodplain) is attributed to longitudinal gradient reduction (from about 1% to about 0.6–0.5%) around Marckoslsheim-Colmar and the huge width of the alluvial plain (15–20 km). The floodplain landscape is also characterized by a multitude of large paleochannels originating from the late glacial braided Rhine system, serving as pre-established pathways for the reoccupation of fluvial systems. In addition, the infilling deposits of these paleochannels, which predominantly consist of sands, are more susceptible to scouring and modification than the adjacent floodplain (e.g., Mohrig et al., 2000). Thus, we expect that these factors promoted recurrent avulsions in the area, primarily through the reoccupation of abandoned channels. Our sedimentological and age data (e.g., showing several geochronological gaps) provide evidence of the successive reoccupation of these late glacial paleochannels by the Rhine and Ill systems, reflecting repeated avulsion episodes throughout the Holocene. Avulsions, primarily occurring through the reoccupation of abandoned channels, represent a common feature in various fluvial systems (Valenza et al., 2020). Avulsion by channel reoccupation has been documented in numerous river systems, including the Brahmaputra River (Bristow, 1999), the lower Saskatchewan River (Morozova and Smith, 1999), the Rhine-Meuse delta (Stouthamer and Berendsen, 2000), the upper Columbia River (Makaske et al., 2002), the Mississippi and Red Rivers (Aslan et al., 2005), and the Baghmati River (Sinha et al., 2005).

The studied section of the URG is tectonically active up till today (Liaghat et al., 1998; Behrmann et al., 2003; Nivière et al., 2008), with active faults spread across the alluvial plain (Behrmann et al., 2003). Consequently, local tectonic movements during the Holocene may have driven avulsion (at least partly)

and lateral movements of the river systems in the valley reach (Bouiflane, 2008). Holocene tectonic activity in the southeastern URG resulted in the formation of a distinct SSW-NNE terrace step (Hochgestade-Tiefgestade), which is exclusively found east of the current Rhine River channel (Frechen et al., 2009; Lämmermann-Barthel et al., 2009). Preferential subsidence caused by this morphological step is believed to have promoted the Rhine's eastward movement across the alluvial plain. Similarly, local tectonic subsidence west of the Ried Noir (Jung et al., 1936; Vogt, 1992; Schmitt et al., 2016) may have favored the movement of the Ill and Fecht Rivers toward a subsiding area in the western portion of the alluvial plain. Several fluvial systems, such as the Andean and foreland rivers in the Amazon basin, the Brahmaputra River, the Tisza River, and the Niger River system, have also shown evidence of avulsions in a preferential direction caused by local tectonic subsidence (Makaske, 2001 and references therein).

Furthermore, the upwelling of a salt diapir that runs from the southeast of Colmar to the north of Marckolsheim (Jung et al., 1936; Liaghat et al., 1998; Lutz and Cleintuar, 1999; Bouiflane, 2008; Supplementary Fig. S2) is also thought to have an influence on the displacement of the Rhine and Ill Rivers in opposing directions. The salt diapir, which is still rising (Liaghat et al., 1998), may have resulted in a local microtopography that triggers avulsions while also pushing the rivers in opposite directions.

Conclusions

A comprehensive analysis of the paleochannel systems in the Ried Central d'Alsace allowed us to reconstruct the long-term temporal trajectory of the fluvial hydrosystems in this reach of the Upper Rhine Valley. The late glacial was dominated by a highly dynamic and laterally mobile Rhine system, whose fluvial dynamics were primarily influenced by climate-related environmental and hydro-geomorphological changes that characterized the period. The comparably braided Fecht system and the nascent Ill River played a lesser role in the fluvial evolution of the region during the late glacial. During the transition from the late glacial to the Holocene, the region's fluvial landscape experienced several significant changes. These included a probable enlargement of the Ill system, a discernible narrowing of the Rhine's active belt, and an evolution in the character of the fluvial systems, with a clear appearance and maintenance of anastomosing channel patterns. This transformative trajectory contrasts sharply with the northern section of the Upper Rhine Valley and most other European fluvial systems, which evolved mainly single-channel meandering systems during the Holocene.

The Rhine and Ill fluvial systems in the investigated region maintained their channel patterns throughout the Holocene while progressively moving to the eastern and western sections of the alluvial plain, respectively. Notably, Holocene fluvial dynamics in this section of the Upper Rhine Valley appear to have been strongly controlled by a complex interplay of factors, including climatic influences and non-climatic mechanisms such as the configuration of the alluvial plain (longitudinal slope, width of the alluvial plain), propensity for flood sedimentation over a large area, and local neotectonic processes. Consequently, the findings of this study enhance our understanding of the long-term fluvial evolution of the entire Upper Rhine Valley. They also have significant implications for disentangling the influence of catchment-specific factors on the development of rivers across northwestern and central Europe, where

Holocene fluvial dynamics have been primarily driven by climate and human-induced (catchment scale) environmental and hydrogeomorphological changes. Furthermore, the findings provide valuable insights into the formation and evolution of anastomosing rivers, notably the metamorphosis from braided to anastomosing channels that we have evidenced for the Rhine, which have been comparatively underresearched compared with other river channel types.

References

Abdulkarim, M., Chapkanski, S., Ertlen, D., Mahmood, H., Obioha, E., Preusser, F., Rambeau, C., Salomon, F., Schiemann, M., Schmitt, L., 2022. Morpho-sedimentary characteristics of Holocene paleochannels in the Upper Rhine alluvial plain, France. *E&G Quaternary Science Journal* **71**, 191–212.

Abdulkarim, M., Grema, H.M., Adamu, I.H., Mueller, D., Schulz, M., Ulbrich, M., Miocic, J.M., Preusser, F., 2021. Effect of using different chemical dispersing agents in grain size analyses of fluvial sediments via laser diffraction spectrometry. *Methods and Protocols* **4**, 44.

Al Siddik, A.M., 1986. Contribution à l'étude de la dynamique de l'humification des sols hydromorphes du Ried Ello-Rhénan (Région d'Illhaeusern, Haut-Rhin). PhD thesis, Nancy 1 University, France.

Al Siddik, A.M., Party, J.-P., Mettauer, H., Schenck, C., Guillet, B., 1989. L'âge des sols et des formations alluviales du Ried ello-rhénan. Exemple d'un secteur test au Sud d'Illhaeusern, Haut-Rhin./The age of soils and alluvial materials of the Central Ried of Alsace. Example of a test area near lllhaeusern, Haut Rhin, France. *Sciences Géologiques Bulletin* **42**, 107–116.

Antoine, P., Munaut, A.-V., Limondin-Lozouet, N., Ponel, P., Dupéron, J., Dupéron, M., 2003. Response of the Selle River to climatic modifications during the Lateglacial and Early Holocene (Somme Basin-northern France). *Quaternary Science Reviews* **22**, 2061–2076.

Arbogast, A.F., Bookout, J.R., Schrotenboer, B.R., Lansdale, A., Rust, G.L., Bato, V.A., 2008. Post-glacial fluvial response and landform development in the upper Muskegon River valley in north-central lower Michigan, U.S.A. *Geomorphology* **102**, 615–623.

Arnaud, F., 2012. Approches géomorphologique historique et expérimentale pour la resturation de la dynamique sédimentaire d'un tronçon fluvial aménagé: le cas su Vieux Rhin entre Kembs et Breisach (France, Allemagne). PhD thesis, University of Lyon, France.

Aslan, A., Autin, W.J., Blum, M.D., 2005. Causes of river avulsion: Insights from the Late Holocene avulsion history of the Mississippi River, U.S.A. *Journal of Sedimentary Research* **75**, 650–664.

Behrmann, J.H., Hermann, O., Horstmann, M., Tanner, D.C., Bertrand, G., 2003. Anatomy and kinematics of oblique continental rifting revealed: a three-dimensional case study of the southeast Upper Rhine graben (Germany). *American Association of Petroleum Geologists Bulletin* **87**, 1105–1121.

Berendsen, H., Hoek, W., Schorn, E., 1995. Late Weichselian and Holocene river channel changes of the rivers Rhine and Meuse in the Netherlands (Land van Maas en Waal). *Paläoklimaforschung* **14**, 151–171.

Birch, G.F., 1981. The Karbonat-Bombe: a precise, rapid and cheap instrument for determining calcium carbonate in sediments and rocks. *Transactions of the Geological Society of South Africa* **84**, 199–203.

Blott, S.J., Pye, K., 2001. GRADISTAT: a grain size distribution and statistics package for the analysis of unconsolidated sediments. *Earth Surface Processes and Landforms* **26**, 1237–1248.

Boës, E., Schmitt, L., Schwartz, D., Gebhardt, A., Goepp, S., Lasserre, M., 2007. L'anthropisation des zones humides de la plaine d'Alsace au cours de la Protohistoire: problématiques d'études à partir des fouilles récentes menées sur les tumulus de Mussig Plaetze (Bas-Rhin). In: Barral, P., Daubigney, A., Dunning, C., Kaenel, G., Roulière-Lambert, M. J. (Eds.), *L'âge du Fer dans l'arc jurassien et ses marges. Dépôts, lieux sacrés et territorialité à l'âge du Fer.* Annales Littéraires, Série "Environnement, sociétés et archéologie." Presses Universitaires de Franche-Comté, Besançon, France, pp. 113–118.

Bos, J.A.A., Dambeck, R., Kalis, A.J., Schweizer, A., Thiemeyer, H., 2008. Palaeoenvironmental changes and vegetation history of the northern Upper Rhine Graben (southwestern Germany) since the Lateglacial. *Netherlands Journal of Geosciences* **87**, 67–90.

Bouiflane, M., 2008. Cartographies aéromagnétique et magnétique multi-échelles:étude structurale d'une région du Fossé rhénan. PhD thesis, University of Strasbourg, France.

Bristow, C.S., 1999. Gradual avulsion, river metamorphosis and reworking by underfit streams: a modern example from the Brahmaputra River in Bangladesh and a possible ancient example in the Spanish Pyrenees. In: Smith, N.D., Rogers, J. (Eds.), *Fluvial Sedimentology VI.* Wiley, Oxford, pp. 221–230.

Bronk Ramsey, C., 2009. Bayesian analysis of radiocarbon dates. *Radiocarbon* **51**, 337–360.

Buylaert, J.P., Murray, A.S., Thomsen, K.J., Jain, M., 2009. Testing the potential of an elevated temperature IRSL signal from K-feldspar. *Radiation Measurements* **44**, 560–565.

Carbiener, R., 1969. Le Grand Ried d'Alsace, Ecologie d'un paysage. *Bulletin de la Societe industrielle de Mulhouse* **1**, 15–44.

Carbiener, R., 1983a. *Brunnenwasser, Encyclopedie de l'Alsace.* Publitotal, Strasbourg.

Carbiener, R., 1983b. Le grand Ried central d'Alsace: ecologie et evolution d'une zone humide d'origine fluviale rhénane. *Bulletin d'écologie* **14**, 249–277.

Carbiener, R., Dillmann, E., 1992. Cas Type de Rhinau-Daubensand: l'évolution du paysage rhénan dans la région de Rhinau, au cœur du secteur des Giessen, des Muhlbach et Brunnenwasser. In: Gallusser, W.A., Schenker, A. (Eds.), *Die Auen am Oberrhein / Les zones alluviales du Rhin supérieur.* Birkhäuser Basel, Basel, pp. 113–136.

Chapkanski, S., Ertlen, D., Rambeau, C., Schmitt, L., 2020. Provenance discrimination of fine sediments by mid-infrared spectroscopy: calibration and application to fluvial palaeo-environmental reconstruction. *Sedimentology* **67**, 1114–1134.

Chardon, V., Schmitt, L., Arnaud, F., Piégay, H., Clutier, A., 2021. Efficiency and sustainability of gravel augmentation to restore large regulated rivers: insights from three experiments on the Rhine River (France/Germany). *Geomorphology* **380**, 107639.

Commission Internationale de l'Hydrologie du Bassin du Rhin, 1977. *Le bassin du Rhin.* Monographie Hydrologique 3. CHR, Utrecht, Netherlands.

[CGIAR-CSI] Consortium for Spatial Information, n.d. SRTM Data (accessed June 13, 2022). https://srtm.csi.cgiar.org/srtmdata.

Dambeck, R., Thiemeyer, H., 2002. Fluvial history of the northern Upper Rhine River (southwestern Germany) during the Lateglacial and Holocene times. *Quaternary International* **93–94**, 53–63.

Dearing, J., 1999. ISBN 0 9523409 0 9*Environmental Magnetic Susceptibility: Using the Bartington MS2 System.* Chi Publications, Kenilworth, UK.

Delile, H., Schmitt, L., Jacob-Rousseau, N., Grosprêtre, L., Privolt, G., Preusser, F., 2016. Headwater valley response to climate and land use changes during the Little Ice Age in the Massif Central (Yzeron basin, France). *Geomorphology* **257**, 179–197.

Depreux, B., Lefèvre, D., Berger, J.-F., Segaoui, F., Boudad, L., El Harradji, A., Degeai, J.-P., Limondin-Lozouet, N., 2021. Alluvial records of the African Humid Period from the NW African highlands (Moulouya basin, NE Morocco). *Quaternary Science Reviews* **255**, 106807.

Druzhinina, O., Kublitskiy, Y., Stančikaitė, M., Nazarova, L., Syrykh, L., Gedminienė, L., Uogintas, D., *et al.*, 2020. The Late Pleistocene–Early Holocene palaeoenvironmental evolution in the SE Baltic region: a new

approach based on chironomid, geochemical and isotopic data from Kamyshovoye Lake, Russia. *Boreas* **49**, 544–561.

Erkens, G., Dambeck, R., Volleberg, K.P., Bouman, M.T.I.J., Bos, J.A.A., Cohen, K.M., Wallinga, J., Hoek, W.Z., 2009. Fluvial terrace formation in the northern Upper Rhine Graben during the last 20000 years as a result of allogenic controls and autogenic evolution. *Geomorphology* **103**, 476–495.

Erkens, G., Hoffmann, T., Gerlach, R., Klostermann, J., 2011. Complex fluvial response to Lateglacial and Holocene allogenic forcing in the Lower Rhine Valley (Germany). *Quaternary Science Reviews* **30**, 611–627.

Ertlen, D., Schwartz, D., Trautmann, M., Webster, R., Brunet, D., 2010. Discriminating between organic matter in soil from grass and forest by near-infrared spectroscopy. *European Journal of Soil Science* **61**, 207–216.

Eschbach, D., Schmitt, L., Imfeld, G., May, J.-H., Payraudeau, S., Preusser, F., Trauerstein, M., Skupinski, G., 2018. Long-term temporal trajectories to enhance restoration efficiency and sustainability on large rivers: an interdisciplinary study. *Hydrology and Earth System Sciences* **22**, 2717–2737.

Faershtein, G., Porat, N., Matmon, A., 2020. Extended-range luminescence dating of quartz and alkali feldspar from aeolian sediments in the eastern Mediterranean. *Geochronology* **2**, 101–118.

Frechen, M., Ellwanger, D., Rimkus, D., Techmer, A., 2009. Timing of medieval fluvial aggradation at Bremgarten in the southern Upper Rhine Graben —a test for luminescence dating. *E&G Quaternary Science Journal* **57**, 411–432.

Gabriel, G., Ellwanger, D., Hoselmann, C., Weidenfeller, M., Wielandt-Schuster, U., 2013. The Heidelberg Basin, Upper Rhine Graben (Germany): a unique archive of Quaternary sediments in Central Europe. *Quaternary International* **292**, 43–58.

Galbraith, R.F., Roberts, R.G., Laslett, G.M., Yoshida, H., Olley, J.M., 1999. Optical dating of single and multiple grains of quartz from Jinmium rock shelter, northern Australia: part I, experimental design and statistical models. *Archaeometry* **41**, 339–364.

Gao, C., Boreham, S., Preece, R.C., Gibbard, P.L., Briant, R.M., 2007. Fluvial response to rapid climate change during the Devensian (Weichselian) Lateglacial in the River Great Ouse, southern England, UK. *Sedimentary Geology* **202**, 193–210.

Haimberger, R., Hoppe, A., Schäfer, A., 2005. High-resolution seismic survey on the Rhine River in the northern Upper Rhine Graben. *International Journal of Earth Sciences* **94**, 657–668.

Han, J., Kim, W., 2022. Linking levee-building processes with channel avulsion: geomorphic analysis for assessing avulsion frequency and channel reoccupation. *Earth Surface Dynamics* **10**, 743–759.

Heiri, O., Lotter, A.F., Lemcke, G., 2001. Loss on ignition as a method for estimating organic and carbonate content in sediments: reproducibility and comparability of results. *Journal of Paleolimnology* **25**, 101–110.

Hinderer, M., 2001. Late Quaternary denudation of the Alps, valley and lake fillings and modern river loads. *Geodinamica Acta* **14**, 231–263.

Hirth, C., 1971. Eléments d'explication à la formation des Rieds ellorhénans au nord de Colmar du début du Post-glaciaire à la canalisation du Rhin au XIXè siècle. *Bulletin de la Société d'histoire naturelle de Colmar* **54**, 21–44.

Hoek, W.Z., Lammertsma, E.I., Bohncke, S.J.P., Bos, J.A.A., Bunnik, F., Kasse, C., Schokker, J., Westerhoff, W., 2017. Lateglacial and early Holocene vegetation development and fluvial system changes in the northern Meuse valley, the Netherlands: a review of palynological data. *Netherlands Journal of Geosciences* **96**, 93–114.

Hoffmann, T., Lang, A., Dikau, R., 2008. Holocene river activity: analysing 14C-dated fluvial and colluvial sediments from Germany. *Quaternary Science Reviews* **27**, 2031–2040.

Holzhauer, I., Kadereit, A., Schukraft, G., Kromer, B., Bubenzer, O., 2017. Spatially heterogeneous relief changes, soil formation and floodplain aggradation under human impact—geomorphological results from the Upper Rhine Graben (SW Germany). *Annals of Geomorphology* **61**, 121–158.

Houben, P., Hoffmann, T., Zimmermann, A., Dikau, R., 2006. Land use and climatic impacts on the Rhine system (RheinLUCIFS): quantifying sediment fluxes and human impact with available data. *Catena* **66**, 42–52.

Huisink, M., 1997. Late-glacial sedimentological and morphological changes in a lowland river in response to climatic change: the Maas, southern Netherlands. *Journal of Quaternary Science* **12**, 209–223.

Huisink, M., 1999. Lateglacial river sediment budgets in the Mass valley, The Netherlands. *Earth Surface Processes and Landforms* **24**, 93–109.

Huntley, D.J., Lamothe, M., 2001. Ubiquity of anomalous fading in K-feldspars and the measurement and correction for it in optical dating. *Canadian Journal of Earth Sciences* **38**, 1093–1106.

Ivy-Ochs, S., Schäfer, J., Kubik, P.W., Synal, H.-A., Schlüchter, C., 2004. Timing of deglaciation on the northern Alpine foreland (Switzerland). *Eclogae Geologicae Helvetiae* **97**, 47–55.

Jung, J., Schlumberger, C., Schlumberger, M., 1936. Soulèvement des alluvions du Rhin par les intrusions salines diapires de la Haute Alsace (Planche IV et IV bis). *Sciences Géologiques* **3**, 77–86.

Kalis, A.J., Merkt, J., Wunderlich, J., 2003. Environmental changes during the Holocene climatic optimum in central Europe—human impact and natural causes. *Quaternary Science Reviews* **22**, 33–79.

Kasse, C., Bohncke, S.J.P., Vandenberghe, J., Gábris, G., 2010. Fluvial style changes during the last glacial–interglacial transition in the middle Tisza valley (Hungary). *Proceedings of the Geologists' Association* **121**, 180–194.

Kasse, C., Hoek, W.Z., Bohncke, S.J.P., Konert, M., Weijers, J.W.H., Cassee, M.L., Van Der Zee, R.M., 2005. Late glacial fluvial response of the Niers-Rhine (western Germany) to climate and vegetation change. *Journal of Quaternary Science* **20**, 377–394.

Kirchner, A., Karaschewski, J., Schulte, P., Wunderlich, T., Lauer, T., 2022. Latest Pleistocene and Holocene floodplain evolution in Central Europe— insights from the Upper Unstrut catchment (NW-Thuringia/Germany). *Geosciences* **12**, 310.

Kirchner, A., Nehren, U., Behling, H., Heinrich, J., 2015. Mid- and late Holocene fluvial dynamics in the tropical Guapi-Macacu catchment, Southeast Brazil: the role of climate change and human impact. *Palaeogeography, Palaeoclimatology, Palaeoecology* **426**, 308–318.

Kock, S., Huggenberger, P., Preusser, F., Rentzel, P., Wetzel, A., 2009. Formation and evolution of the Lower Terrace of the Rhine River in the area of Basel. *Swiss Journal of Geosciences* **102**, 307–321.

Kolstrup, E., 1980. Climate and stratigraphy in northwestern Europe between 30,000 BP and 13,000 BP, with special reference to The Netherlands. *Mededelingen Rijks Geologische Dienst* **32**(15), 181–253.

Kremer, M., Rieb, J.-P., Rebholtz, C., Delecolle, J.-C., 1978. Écologie des Cératopogonidés de la plaine d'Alsace: I. - Le genre *Culicoides* des sols humides du Ried. *Annales de Parasitologie* **53**, 101–115.

Kreutzer, S., Burow, C., Dietze, M., Fuchs, M. C., Schmidt, C., Fischer, M., Friedrich, J., Riedesel, S., Autzen, M., Mittelstrass, D., 2020. Luminescence: comprehensive luminescence dating data analysis, R package version 0.9.23. https://CRAN.R-project.org/package=Luminescence.

Lämmermann-Barthel, J., Neeb, I., Hinderer, M., Frechen, M., 2009. Last glacial to Holocene fluvial aggradation and incision in the southern Upper Rhine graben: climatic and neotectonic controls. *Quaternaire* **20**, 25–24.

Lang, A., Bork, H.-R., Mäckel, R., Preston, N., Wunderlich, J., Dikau, R., 2003. Changes in sediment flux and storage within a fluvial system: some examples from the Rhine catchment. *Hydrological Processes* **17**, 3321–3334.

Liaghat, C., Villemin, T., Jouanne, F., 1998. Déformation verticale actuelle dans la partie sud du fossé d'Alsace (France). *Comptes Rendus de l'Académie des Sciences, Series IIA, Earth and Planetary Science* **327**, 55–60.

Lowe, J.J., Walker, M., 2014. *Reconstructing Quaternary Environments*, 3rd ed. Routledge, London.

Lutz, M., Cleintuar, M., 1999. Geological results of a hydrocarbon exploration campaign in the southern Upper Rhine Graben (Alsace Centrale, France), *Bulletin für Angewandte Geologie* **4**, 3–80.

Mäckel, R., 1998. Flußaktivität und Talgeschichte des Spät- und Postglazials im Oberrheintiefland und Schwarzwald. In: Mäckel, R., Friedmann, A. (Eds.), *Wandel der Geo-Biosphäre in den letzten 15000 Jahren im südlichen Oberrheintiefland und Schwarzwald.* Freiburger Geographische Hefte 54. Institut für Physische Geographie der Albert-Ludwigs-Universität, Freiburg im Bresigau, pp. 31–50.

Mäckel, R., Friedmann, A., Sudhaus, D., 2009. Environmental changes and human impact on landscape development in the Upper Rhine region. *Erdkunde* **63**, 35–49.

Makaske, B., 2001. Anastomosing rivers: a review of their classification, origin and sedimentary products. *Earth Science Reviews* **53**, 149–196.

Makaske, B., Smith, D.G., Berendsen, H.J.A., 2002. Avulsions, channel evolution and floodplain sedimentation rates of the anastomosing upper Columbia River, British Columbia, Canada. *Sedimentology* **49**, 1049–1071.

Martin, H.K., Edmonds, D.A., 2022. The push and pull of abandoned channels: how floodplain processes and healing affect avulsion dynamics and alluvial landscape evolution in foreland basins. *Earth Surface Dynamics* **10**, 555–579.

May, J.-H., Marx, S.K., Reynolds, W., Clark-Balzan, L., Jacobsen, G.E., Preusser, F., 2018. Establishing a chronological framework for a late Quaternary seasonal swamp in the Australian "Top End." *Quaternary Geochronology* **47**, 81–92.

Meylemans, E., Bogemans, F., Storme, A., Perdaen, Y., Verdurmen, I., Deforce, K., 2013. Lateglacial and Holocene fluvial dynamics in the Lower Scheldt basin (N-Belgium) and their impact on the presence, detection and preservation potential of the archaeological record. *Quaternary International* **308–309**, 148–161.

Mohrig, D., Heller, P.L., Paola, C., Lyons, W.J., 2000. Interpreting avulsion process from ancient alluvial sequences: Guadalope-Matarranya system (northern Spain) and Wasatch Formation (western Colorado). *Geological Society of America Bulletin* **112**, 1787.

Mol, J., Vandenberghe, J., Kasse, C., 2000. River response to variations of periglacial climate in mid-latitude Europe. *Geomorphology* **33**, 131–148.

Morozova, G.S., Smith, N.D., 1999. Holocene Avulsion History of the Lower Saskatchewan Fluvial System, Cumberland Marshes, Saskatchewan–Manitoba, Canada. In: Smith, N.D., Rogers, J. (Eds.), *Fluvial Sedimentology VI*. Wiley, Oxford, pp. 231–249.

Müller, G., Gastner, M., 1971. The "Karbonat-Bombe," a simple device for the determination of carbonate content in sediment, soils, and other materials. *Neues Jahrbuch für Mineralogie* **10**, 466–469.

Murray, A.S., Wintle, A.G., 2000. Luminescence dating of quartz using an improved single-aliquot regenerative-dose protocol. *Radiation Measurements* **32**, 57–73.

Nanson, G.C., Knighton, A.D., 1996. Anabranching rivers: their cause, character and classification. *Earth Surface Processes and Landforms* **21**, 217–239.

Nivière, B., Bruestle, A., Bertrand, G., Carretier, S., Behrmann, J., Gourry, J.-C., 2008. Active tectonics of the southeastern Upper Rhine Graben, Freiburg area (Germany). *Quaternary Science Reviews* **27**, 541–555.

Ollive, V., Petit, C., Garcia, J.-P., Reddé, M., 2006. Rhine flood deposits recorded in the Gallo-Roman site of Oedenburg (Haut-Rhin, France). *Quaternary International* **150**, 28–40.

Plotzki, A., May, J.-H., Preusser, F., Roesti, B., Denier, S., Lombardo, U., Veit, H., 2015. Geomorphology and evolution of the late Pleistocene to Holocene fluvial system in the south-eastern Llanos de Moxos, Bolivian Amazon. *Catena* **127**, 102–115.

Prescott, J.R., Hutton, J.T., 1994. Cosmic ray contributions to dose rates for luminescence and ESR dating: large depths and long-term time variations. *Radiation Measurements* **23**, 497–500.

Preusser, F., 2008. Characterisation and evolution of the River Rhine system. *Netherlands Journal of Geosciences* **87**, 7–19.

Preusser, F., Büschelberger, M., Kemna, H.A., Miocic, J., Mueller, D., May, J.-H., 2021. Exploring possible links between Quaternary aggradation in the Upper Rhine Graben and the glaciation history of northern Switzerland. *International Journal of Earth Sciences* **110**, 1827–1846.

Preusser, F., Degering, D., Fuchs, M., Hilgers, A., Kadereit, A., Klasen, N., Krbetschek, M., Richter, D., Spencer, J.Q.G., 2008. Luminescence dating: basics, methods and applications. *E&G Quaternary Science Journal* **57**, 95–149.

Preusser, F., May, J.-H., Eschbach, D., Trauerstein, M., Schmitt, L., 2016. Infrared stimulated luminescence dating of 19th century fluvial deposits from the Upper Rhine River. *Geochronometria* **43**, 131–142.

Reimer, P.J., Austin, W.E.N., Bard, E., Bayliss, A., Blackwell, P.G., Bronk Ramsey, C., Butzin, M., et al., 2020. The IntCal20 Northern Hemisphere radiocarbon age calibration curve (0–55 cal kBP). *Radiocarbon* **62**, 725–757.

Richter, D., Richter, A., Dornich, K., 2015. *Lexsyg smart*—a luminescence detection system for dosimetry, material research and dating application. *Geochronometria* **42**, 202–209.

Roberts, H.M., Durcan, J.A., Duller, G.A.T., 2009. Exploring procedures for the rapid assessment of optically stimulated luminescence range-finder ages. *Radiation Measurements* **44**, 582–587.

Schirmer, W., Bos, J.A., Dambeck, R., Hinderer, M., Preston, N., Schulte, A., Schwalb, A., Wessels, M., 2005. Holocene fluviatile processes and valley history in the River Rhine catchment. *Erdkunde* **59**, 199–215.

Schmitt, L., 2001. Typologie hydro-géomorphologique fonctionnelle de cours d'eau: recherche méthodologique appliquée aux systems fluviaux d'Alsace. PhD thesis, University of Strasbourg, France.

Schmitt, L., Beisel, J.N., Preusser, F., de Jong, C., Wantzen, K.M., Chardon, V., Staentzel, C., et al., 2019. Sustainable management of the Upper Rhine River and its alluvial plain: Lessons from interdisciplinary research in France and Germany. In: Hamman, P., Vuilleumier, S. (Eds.), *Sustainability Research in the Upper Rhine Region, Concepts and Case Studies*. Presses Universitaires de Strasbourg, Strasbourg, pp. 201–226.

Schmitt, L., Houssier, J., Martin, B., Beiner, M., Skupinski, G., Boës, E., Schwartz, D., et al., 2016. Paléo-dynamique fluviale holocène dans le compartiment sud-occidental du fossé rhénan (France). *Revue Archéologique de l'Est* **42**, 15–33.

Schmitt, L., Lafont, M., Trémolières, M., Jezequel, C., Vivier, A., Breil, P., Namour, P., Valin, K., Valette, L., 2011. Using hydro-geomorphological typologies in functional ecology: Preliminary results in contrasted hydrosystems. *Physics and Chemistry of the Earth, Parts A/B/C* **36**, 539–548.

Schmitt, L., Maire, G., Nobelis, P., Humbert, J., 2007. Quantitative morphodynamic typology of rivers. A methodological study based on the French Upper Rhine basin. *Earth Surface Processes and Landforms* **32**, 1726–1746.

Schneider, R., 2000. Landschafts- und Umweltgeschichte im Einzugsgebiet der Elz. PhD thesis, University of Freiburg, Germany.

Schulze, T., Schwahn, L., Fülling, A., Zeeden, C., Preusser, F., Sprafke, T., 2022. Investigating the loess–palaeosol sequence of Bahlingen-Schönenberg (Kaiserstuhl), southwestern Germany, using a multi-methodological approach. *E&G Quaternary Science Journal* **71**, 145–162.

Schumm, S.A., Dumont, J.F., Holbrook J.M., 2000. *Active Tectonics and Alluvial Rivers*. Cambridge University Press, New York.

Sinha, R., Gibling, M.R., Jain, V., Tandon, S.K., 2005. Sedimentology and avulsion patterns of the anabranching Baghmati River in the Himalayan foreland basin, India. In: Blum, M.D., Marriott, S.B., Leclair, S.F. (Eds.), *Fluvial Sedimentology VII*. Wiley, Oxford, pp. 181–196.

Slingerland, R., Smith, N.D., 2004. River avulsions and their deposits. *Annual Review of Earth and Planetary Sciences* **32**, 257–285.

Stouthamer, E., Berendsen, H.J.A., 2000. Factors controlling the Holocene avulsion history of the Rhine-Meuse Delta (The Netherlands). *Journal of Sedimentary Research* **70**, 1051–1064.

Stouthamer, E., Berendsen, H.J.A., 2007. Avulsion: the relative roles of autogenic and allogenic processes. *Sedimentary Geology* **198**, 309–325.

Thiel, C., Buylaert, J.-P., Murray, A., Terhorst, B., Hofer, I., Tsukamoto, S., Frechen, M., 2011. Luminescence dating of the Stratzing loess profile (Austria)—testing the potential of an elevated temperature post-IR IRSL protocol. *Quaternary International* **234**, 23–31.

Törnqvist, T.E., 1998. Longitudinal profile evolution of the Rhine-Meuse system during the last deglaciation: interplay of climate change and glacio-eustasy? *Terra Nova* **10**, 11–15.

Törnqvist, T.E., 1994. Middle and late Holocene avulsion history of the River Rhine (Rhine-Meuse delta, Netherlands). *Geology* **22**, 711.

Trémolières, M., Eglin, I., Roeck, U., Carbiener, R., 1993. The exchange process between river and groundwater on the Central Alsace floodplain (eastern France): I. The case of the canalised river Rhine. *Hydrobiologia* **254**, 133–148.

Valenza, J.M., Edmonds, D.A., Hwang, T., Roy, S., 2020. Downstream changes in river avulsion style are related to channel morphology. *Nature Communications* **11**, 2116.

Vandenberghe, J., 1995. Timescales, climate and river development. *Quaternary Science Reviews* **14**, 631–638.

Vandenberghe, J., Kasse, C., Bohncke, S., Kozarski, S., 1994. Climate-related river activity at the Weichselian-Holocene transition: a comparative study of the Warta and Maas rivers. *Terra Nova* **6**, 476–485.

Vayssière, A., Rué, M., Recq, C., Gardère, P., Thamó-Bozsó, E., Castanet, C., Virmoux, C., Gautier, E., 2019. Lateglacial changes in river morphologies of northwestern Europe: An example of a smooth response to climate forcing (Cher River, France). *Geomorphology* **342**, 20–36.

Vogt, H., 1992. *Le relief en Alsace: étude géomorphologique du rebord sud-occidental du Fossé rhenan.* Librairie Oberlin, Strasbourg.

von Suchodoletz, H., Menz, M., Kühn, P., Sukhishvili, L., Faust, D., 2015. Fluvial sediments of the Algeti River in southeastern Georgia—an archive of Late Quaternary landscape activity and stability in the Transcaucasian region. *Catena* **130**, 95–107.

Wessels, M., 1998. Natural environmental changes indicated by Late glacial and Holocene sediments from Lake Constance, Germany. *Palaeogeography, Palaeoclimatology, Palaeoecology* **140**, 421–432.

Wintle, A.G., Murray, A.S., 2006. A review of quartz optically stimulated luminescence characteristics and their relevance in single-aliquot regeneration dating protocols. *Radiation Measurements* **41**, 369–391.

Ziegler, P.A., 1992. European Cenozoic rift system. *Tectonophysics* **208**, 91–111.

Zielhofer, C., Faust, D., Linstädter, J., 2008. Late Pleistocene and Holocene alluvial archives in the Southwestern Mediterranean: changes in fluvial dynamics and past human response. *Quaternary International* **181**, 39–54.